THE UNIVERSITY of EDINBURGH

Edinburgh Research Explorer

# Lateral thinking – interocular symmetry and asymmetry in neurovascular patterning, in health and disease

**Citation for published version:**
Cameron, J, Megaw, R, Tatham, A, McGrory, S, MacGillivray, T, Doubal, F, Wardlaw, J, Trucco, E, Chandran, S & Dhillon, B 2017, 'Lateral thinking – interocular symmetry and asymmetry in neurovascular patterning, in health and disease', *Progress in Retinal and Eye Research*. https://doi.org/10.1016/j.preteyeres.2017.04.003

**Digital Object Identifier (DOI):**
10.1016/j.preteyeres.2017.04.003

**Link:**
Link to publication record in Edinburgh Research Explorer

**Document Version:**
Peer reviewed version

**Published In:**
Progress in Retinal and Eye Research

**Publisher Rights Statement:**
This is author's peer-reviewed manuscript as accepted for publication

**General rights**
Copyright for the publications made accessible via the Edinburgh Research Explorer is retained by the author(s) and / or other copyright owners and it is a condition of accessing these publications that users recognise and abide by the legal requirements associated with these rights.

**Take down policy**
The University of Edinburgh has made every reasonable effort to ensure that Edinburgh Research Explorer content complies with UK legislation. If you believe that the public display of this file breaches copyright please contact openaccess@ed.ac.uk providing details, and we will remove access to the work immediately and investigate your claim.

OPEN ACCESS

Download date: 04. May. 2023

# Lateral thinking – interocular symmetry and asymmetry in neurovascular patterning, in health and disease

James R. Cameron [a, b, *]
Roly D. Megaw [c, d]
Andrew J. Tatham [d]
Sarah McGrory [b]
Thomas J. MacGillivray [b, e]
Fergus N. Doubal [b]
Joanna M. Wardlaw [b]
Emanuele Trucco [f]
Siddharthan Chandran [a, b]
Baljean Dhillon [b, d]

[a] Anne Rowling Regenerative Neurology Clinic, University of Edinburgh, Chancellor's Building, 49 Little France Crescent, Edinburgh, EH16 4SB, UK

[b] Centre for Clinical Brain Sciences, University of Edinburgh, Chancellor's Building, 49 Little France Crescent, Edinburgh, EH16 4SB, UK

[c] Scottish Centre for Regenerative Medicine, University of Edinburgh, 5 Little France Drive, Edinburgh, EH16 4UU, UK

[d] Princess Alexandra Eye Pavilion, Chalmers Street, Edinburgh, EH3 9HA, UK

[e] VAMPIRE project, Clinical Research Imaging Centre, University of Edinburgh, Queen's Medical Research Institute, 47 Little France Crescent, Edinburgh, EH16 4TJ, UK

[f] VAMPIRE project, Computer Vision and Image Processing Group, School of Science and Engineering (Computing), University of Dundee, Queen Mother Building, Dundee, DD1 4HN, UK

*** Corresponding Author**
Dr. James R Cameron
Anne Rowling Regenerative Neurology Clinic, University of Edinburgh
Tel: +44 (0)131 465 9500
Email: james.cameron@ed.ac.uk

# Contents

## Abstract

No biological system or structure is likely to be perfectly symmetrical, or have identical right and left forms. This review explores the evidence for eye and visual pathway asymmetry, in health and in disease, and attempts to provide guidance for those studying the structure and function of the visual system, where recognition of symmetry or asymmetry may be essential.

The principal question with regards to asymmetry is not 'are the eyes the same?', for some degree of asymmetry is pervasive, but 'when are they importantly different?'. Knowing if right and left eyes are 'importantly different' could have significant consequences for deciding whether right or left eyes are included in an analysis or for examining the association between a phenotype and ocular parameter. The presence of significant asymmetry would also have important implications for the design of normative databases of retinal and optic nerve metrics.

In this review, we highlight not only the universal presence of asymmetry, but provide evidence that some elements of the visual system are inherently more asymmetric than others, pointing to the need for improved normative data to explain sources of asymmetry and their impact on determining associations with genetic, environmental or health-related factors and ultimately in clinical practice.

## Acknowledgements

JC is supported by a Rowling Scholarship from the Anne Rowling Regenerative Neurology Clinic, University of Edinburgh. AT is supported with an NHS Research Scotland (NRS) Fellowship. FD is supported by a joint Stroke Association/Garfield Weston Foundation Senior Clinical Fellowship. The VAMPIRE team acknowledges support from ESPRC grant SIDD EP/M005976/1 "Multimodal retinal biomarkers for vascular dementia". Part of this research has been conducted using the UK Biobank Resource.

# List of Abbreviations

| | |
|---|---|
| ALKB | alkylated DNA repair protein B |
| ARMD | age-related macular degeneration |
| AVR | arteriole-to-venule ratio |
| BMO | Bruch's membrane opening |
| BMP | bone morphogenetic protein |
| BOLD-MRI | blood oxygenation level dependent magnetic resonance imaging |
| CCA | common carotid artery |
| CI | confidence interval |
| cpRNFL | circumpapillary retinal nerve fibre layer |
| CRAE | central retinal arteriolar equivalent |
| CRVE | central retinal venular equivalent |
| CNV | choroidal neovascular membrane |
| CT | computed tomography |
| Cyc | cyclops |
| DOA | Autosomal dominant optic atrophy |
| ENU | N-ethyl-N-nitrosourea |
| GA | geographic atrophy |
| GCC | ganglion cell complex |
| GCL | ganglion cell layer |
| GC-IPL | ganglion cell and inner plexiform layer |
| HRT | Heidelberg Retina Tomograph |
| ICA | internal carotid artery |
| ICC | intraclass correlation coefficient |
| INL | inner nuclear layer |
| IOP | intraocular pressure |
| LGN | lateral geniculate nucleus |
| LHON | Leber hereditary optic neuropathy |
| MRI | magnetic resonance imaging |
| MS | multiple sclerosis |
| OCT | optical coherence tomography |
| Oep | one-eyed pinhead |
| ONSD | optic nerve sheath diameter |
| OTX | orthodenticle homeobox |
| Pax | paired box protein |
| PCA | posterior cerebral artery |
| Pitx | paired-like homeodomain transcription factor |
| PPAA | posterior pole asymmetry analysis |
| Ptdsr | phosphatidylserine receptor |

| | |
|---|---|
| RAPD | relative afferent pupillary defect |
| RGC | retinal ganglion cell |
| RNFL | retinal nerve fibre layer |
| RP | retinitis pigmentosa |
| RRD | rhegmatogenous retinal detachment |
| SD-OCT | spectral-domain optical coherence tomography |
| SLO | scanning laser ophthalmoscope |
| Sox | SRY-Box transcription factor |
| TBX | T-box transcription factor |
| TCD | transcranial Doppler ultrasonography |
| TD-OCT | time-domain optical coherence tomography |
| TGFβ | transforming growth factor β |
| TMX | thioredoxin-related transmembrane protein |
| USH2A | usherin gene |
| VAMPIRE | vessel assessment and measurement platform for images of the retina |
| WMH | white matter hyperintensities |
| Wnt | wingless-related integration site |

# 1. Introduction

## *1.1. Reflections*

Symmetry is observed in much of biology, with many plants and animals demonstrating some degree of symmetry of anatomical structure. The symmetry observed can be defined as two or more matching regions, identical (or nearly identical) by either mirror or rotational reflection. As humans, we are familiar with our gross anatomical symmetry, but also the important asymmetries within us.

Clinically, we expect our eyes and visual systems to behave somewhat symmetrically. The visual system is designed to be fully bilaterally integrated and this is essential for full field vision. We also observe a pattern of symmetry in many (but not all) ocular diseases, further emphasising the convergence of the two halves of our visual pathway.

However, unanswered questions remain about the pathophysiology of diseases, in those that affect one, and both eyes. In addition, assumptions are made about the symmetry of the eyes in research, for example in studies that analyse retinal vascular morphology. These assumptions may not be correct, and in fact, there may be a consistent pattern of asymmetry between our eyes and visual pathways.

We now have access to tools that are providing increasingly precise measures of ocular structure, such as optical coherence tomography (OCT) of the retina, and automated software analysis of the retinal vascular morphology revealed by fundus imaging. We can therefore begin to challenge assumptions of anatomical symmetry by analysis of sophisticated ocular measurements from large studies utilising these tools.

Simultaneously, clues to the patterning of the neuroretina are emerging from advances in developmental genetics, with immediate relevance to our understanding of the pathology of ocular disease, as well as how we use statistics to investigate the impact of new treatments on these diseases. Indeed, interocular asymmetry is likely not to be simply a statistical difference at a threshold of measurement discrimination, but an important and adaptive property of our visual system.

*1.2. The birds and bees*

In terms of species-specific adaptation in sensory organ asymmetry, birds and bees show a shift in mirror image patterning of structure and function of sensory organs as an evolutionary mechanism to refine head position in relation to the environment. An examination of these deviations from bilaterian patterning sheds insight on how other species differences might arise and suggests subtle variations in symmetry observed in sensory perception of other species might confer a functional and possibly a survival benefit.

By analogy, ocular dominance might also be considered adaptive and for the purposes of this paper this functional difference between the eyes highlights the flaw in assuming that eye symmetry is the rule, rather than the exception. If so, the differences in ocular metrics between our eyes that give rise to refractive differences (and thus confer monovision capability) might be beneficial and mitigate against attempts to correct refractive error. However, this is at the cost of optimal stereopsis which risks interference with visual development, and resulting suppression which becomes maladaptive in the amblyopic individual.

Certainly, the bird or bee with species-specific amblyopia would find it a challenge surviving and reproducing in their natural surroundings. The humble honeybee *Apis mellifera* boasts a brain of fewer than a million neurons yet is capable of complex cognitive tasks (Giurfa et al., 2001). Extensive studies of the main sensory input mediated by the bee antennae and differential specialisation between right and left sides of the brain have revealed lateralisation in olfaction and visual responses (Frasnelli, 2013; Letzkus et al., 2008). The right antenna is more specialised than the left for learning about novel odours and mediating inter-bee interactions and appropriate social responses, and they are better at responding to a visual object when using their right eye.

In vertebrate eyes the assumption that the visual system is based on anatomic symmetry between the two eyes has been challenged. For example, Hart and colleagues reported that the retinae of the European starling, *Sturnus vulgaris* show differences in photoreceptor distribution between right and left eyes associated with lateralisation of visually mediated behaviour (Hart et al., 2000). This interocular anatomic difference is consistent with behavioural observation that birds use right and left eyes preferentially depending on the environmental context. Wiltschko, having previously described the magnetoception of birds being light-mediated (Wiltschko and Wiltschko, 1988), later demonstrated extreme asymmetry in the sensing of magnetic fields that develops over time, with the right eye assuming dominance which is reflected in cerebral lateralisation (Wiltschko et al., 2002).

These structural and functional examples seen in birds and bees suggest that the dogma of assumed symmetry in the human visual system should be re-visited if only to shed light on how best to interpret findings derived from paired datasets in ophthalmic metrics in health and disease, or where only one eye has been measures and assumed to be representative of both.

# 2. Embryology and eye development

## *2.1. Lateral patterning in embryogenesis*

Cells and tissues are instructed, via various epigenetic and genetic cascades, as to their left or right identity at an early stage of embryonic development. The process begins in the embryonic node with the directional vortical movement of node cilia and manifests in numerous left-right asymmetries in the placement of visceral organs (Kawakami et al., 2005). Studies into the left-right axis were originally provided by pharmacological agents that caused asymmetrical developmental defects. Of interest were certain studies that showed extensive limb defects favoured one side over the other, suggesting subtle molecular differences may exist between organs that were otherwise assumed to be symmetrical. This is reflected in certain human syndromes, like the *TBX5*-related Holt-Oram syndrome, where upper limb defects are much more common on the left-hand side than the right (Newbury-Ecob et al., 1996). Craniofacial asymmetry can also result from developmental defects, with the left ear being predominantly under-formed in the *Sox3*-/- mouse (Rizzoti and Lovell-Badge, 2007). There are, indeed, myriad birth defects that demonstrate laterality (Paulozzi and Lary, 1999) and whilst these are congenital in nature, the observation that hemihypertrophy (an intrinsic congenital growth excess resulting in one half of the body being larger than the other) can increase in adulthood suggests that this asymmetrical identity is retained at a cellular level postnatally (Leung et al., 2002).

The brain is well known to be asymmetrical and there is a school of thought that two separate organiser nodes (determining left-right lateralisation) exist; one for the head and one for the body (Levin, 2005). In keeping with this, individuals with *situs inversus* often retain the language lateralisation seen in the majority of right-handed normal individuals (Kennedy et al., 1999) as well as the same incidence of left-handedness as seen in the rest of the population (Torgersen, 1950). The study of non-conjoined monozygotic twins supports this, particularly those determined ‘bookend’ twin pairs. These twins, who manifest mirror image asymmetry, do not display the gross visceral laterality defects that occur in conjoined twins. Rather, they display many subtler kinds of mirror-image asymmetry. These vary from hand preference to hair whorl direction and tooth patterns (Levin, 2005), but interestingly they only seem to manifest features involving the head. So there is a strong body of evidence to suggest that the brain develops asymmetrically. Whilst much less is known about the eye, bookend twins can develop mirrored myopic anisometropia (Okamoto et al., 2001) and optic nerve dysplasia (Cidis et al., 1997). The question, then, is how symmetrically do our eyes develop?

Flatfishes are the most asymmetrical vertebrate; during metamorphosis from a symmetrical larval to the juvenile state the body alters dramatically. Of note, eye migration leads to the eyes being positioned on one side (ocular) only, with no eyes on the blind side. The hard cranial tissues twist in the same direction as the migrating 'blind' eye, with an increase in skin thickness giving rise to the pseudomesial bar (a unique bone to the flatfish), possibly aiding migration. Further, the retro-orbital vesicle is much larger behind the blind eye (Okada et al., 2001). The same appears true in reptiles (Werner and Seifan, 2006) and birds also show ocular asymmetry (Hart et al., 2000). To determine whether mammalian eyes develop asymmetrically, an understanding of early oculogenesis is required.

### *2.2. Mammalian eye development*

In early embryogenesis, shortly after gastrulation, an area of neuroectoderm (the neural plate) forms from the ectoderm germ layer. This process is strongly inhibited by Transforming Growth Factor β (*TGFβ*) signalling pathways (Activin/Nodal and Bone Morphogenetic Protein (*BMP*)) (Chambers et al., 2009; Lupo et al., 2014; Wilson and Edlund, 2001). Subsequent rostrocaudal regionalisation of the neural plate leads to primitive forebrain, midbrain, hindbrain, and spinal cord formation. Again, *BMP* antagonists (produced by the organiser/node) (Wilson and Edlund, 2001) help establish a forebrain (Bachiller et al., 2000). Finally, establishment of transcription factor gradients (such as the Wingless-related integration site (*Wnt*)) leads to patterning of forebrain structures (Heisenberg et al., 2001; Houart et al., 2002).

Following this early patterning, a patch of neuroepithelium within the midline of the presumptive forebrain arises with an eye identity; the 'eye field'. Initially it is a single eye field, but One Eyed Pinhead (*Oep*), released by the prechordal mesoderm, allows the formation of bilateral, symmetrical, primitive eyes. *Oep* down-regulates Cyclops (*cyc*) that in turn leads to a down-regulation of *Pax6* and *ET/TBX3* in the anterior neural plate midline (Li et al., 1997). This midline down-regulation splits the eye field into a left and right domain (Macdonald et al., 1995). The midline then gives rise to ventral forebrain. *Cyc* or *Oep* mutations lead to the cyclops developmental abnormality and the failure of ventral forebrain formation (Hatta et al., 1991). Following successful establishment of bilateral eye fields, the forming of ocular structure can ensue (Figure 1).

Prior to the emergence of the 3-dimensional primitive eye, dorsoventral patterning of each eye field parcels specific areas into progenitor domains committed to forming certain structures, such as the retina and the optic stalk. Specifically, *PAX2* and *PAX6* are essential in establishing this

proximo-ventral character (Megaw et al., 2013; Schwarz et al., 2000). Once eye field patterning has occurred, a cascade of transcription factors (the description of which are beyond the scope of this article) instruct optic grooves to protrude from the rostral forebrain, leading to optic vesicles that extend towards the overlying, non-neural surface ectoderm (Belecky-Adams et al., 1997; Bovolenta et al., 1998; Burmeister et al., 1996; Chow et al., 1999; Chuang and Raymond, 2001; Ferda Percin et al., 2000; Furukawa et al., 1997; Grindley et al., 1995; Liu et al., 1994; Loosli et al., 1999; Mathers et al., 1997; Porter et al., 1997; Wallis et al., 1999; Zuber et al., 1999). Vesicle invagination forms the double layered optic cups, encapsulating surface ectoderm in the process to form the early lens placode. This process requires a highly controlled sequence of transcription factor expression and some evidence from human disease suggests that a certain amount of laterality exists in this process.

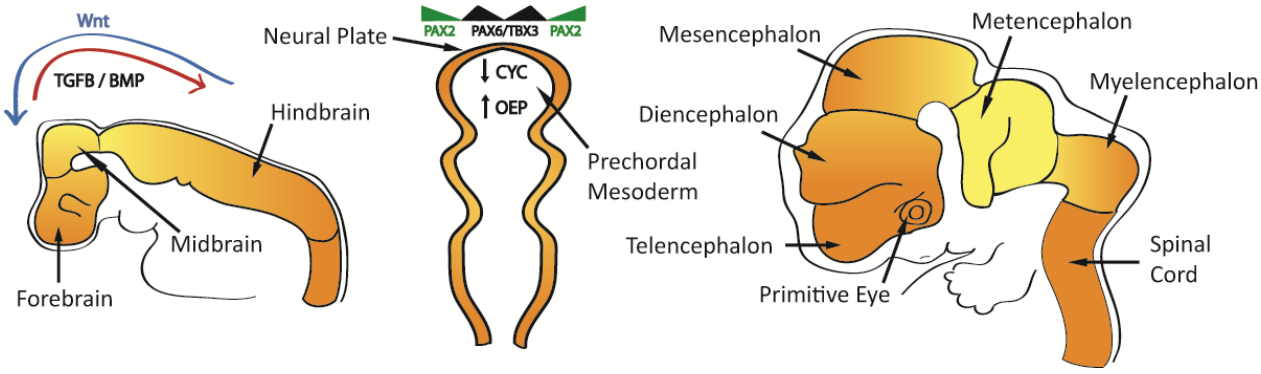


**Figure 1.** Early eye development and signalling pathways

*2.3. Asymmetrical human developmental disease*

Mutations in genes involved in early oculogenesis often result in profound defects. Microphthalmia is a congenital defect that results from reduction in prenatal ocular growth, whereas anophthalmia is the total absence of an eye. They are often a bilateral phenomenon, yet those inherited in an autosomal recessive manner can develop asymmetric or even unilateral disease, even in monozygotic twins (Fleckenstein and Maumenee, 2005). *Sox2*, a member of the high mobility group domain transcription factor family, is involved in maintaining pluripotency but also appears crucial for eye development. Mutations can result in asymmetrical ocular defects varying from micro- to anophthalmia (Fantes et al., 2003) with some patients even displaying a normal contralateral eye (Schneider et al., 2009).

Similarly, the Bone Morphogenic Protein 4 (*BMP4*; part of a family related to the Transforming Growth Factor-beta Proteins) is involved early in embryogenesis and mutations lead to various ocular, digital and brain abnormalities including the SHORT (short stature, hyperextensibility, hernia, ocular depression, Rieger anomaly, and teething delay) syndrome (Reis et al., 2011). Several of the patients described exhibit marked laterality of their disease. Of note, its location on chromosome 14 is near *OTX2*; a well-established cause of asymmetric micro-/anophthalmia. Again, mutations in *OTX2* often manifest with unilateral or asymmetrical disease (Ragge et al., 2005). Mutations in Thioredoxin domain-containing 10 (*TMX3*), expressed in the developing eye, leads to unilateral microphthalmia (Chao et al., 2010) and a maternally-inherited chromosomal deletion containing *TMX3* produced a late-presenting diaphragmatic hernia and unilateral microphthalmia (Zayed et al., 2010). Surprisingly therefore, *TMX3* zebrafish morpholinos result in a bilateral reduction in eye size; suggesting that alternate genes could compensate for reduced *TMX3* gene dosage. There are however, other animal models of developmental disease that do lead to asymmetrical phenotypes.

### *2.4. Asymmetrical development in animal models*

*ALKB* is a 2-oxoglutarate- and iron-dependent dioxygenase that reverses alkylated DNA damage by oxidative demethylation. Its mouse homologue (*Alkbh*) is believed to play a role in epigenetic regulation. *Alkbh1*-deficient mice are not viable but embryologically they display microphthalmia and anophthalmia. Morphologically the microphthalmic eyes are aphakic or have a small, displaced lens with loss of lamination of (swollen) lens fibre cells and vacuoles throughout. Retina is disorganised and dysplastic with rod and cone inclusions surrounded by outer nuclear layer cells, forming rosettes. Thickened, ectopic RPE is evident inside the eye. This suggests *Alkbh1* plays a role in eye development and, interestingly, the phenotype affects the right eye, suggesting a role for *Alkbh1* in ocular lateralization (Nordstrand et al., 2010). Absence of the phosphatidylserine receptor (*Ptdsr*), previously implicated in the recognition and engulfment of apoptotic cells by phagocytes, was shown to result in mainly unilateral anophthalmia (Böse et al., 2004).

Animal models of left-right mispatterning also exhibit ocular phenotypes. *Pitx2* appears to provide ‘leftness’ for pulmonary primordia. Interestingly it is mutated in Reiger syndrome, an autosomal dominant condition characterized by anterior segment dysgenesis. In keeping, the *Pitx2*-/- mouse lacks a corneal endothelium (resulting in anterior segment dysgenesis). That said, while *Pitx2* instructs left-right asymmetry and periocular mesenchyme development, no left-right

eye asymmetry is documented in the knock-out mouse (Lu et al., 1999). A forward ENU-mutational screen produced a series of 'gasping' mice, who displayed a complex syndrome with defects seen in left-right patterning, cardiac development, neural tube closure, limb patterning, eye patterning and anterior gut patterning (Ermakov et al., 2009). Retinal pigment epithelium distribution was abnormal in the embryonic mice with coloboma development in some. Interestingly, cilia formation in the embryonic node was abnormal. Primary cilia are seen as crucial in defining a left-right axis in normal development and, of course, modified primary cilium form the basis of photoreceptor morphology. However, no comment was made on left-right eye asymmetry.

### *2.5. Is normal eye development asymmetrical?*

In summary, although there is a school of thought that organiser nodes may determine left-right lateralisation for the head (Levin, 2005), and evidence points to ocular development in mammals being symmetrical from formation of a midline solitary 'eye field' that divides into right and left (presumed symmetrical) structures (Li et al., 1997; Macdonald et al., 1995), no studies have actually examined whether normal eye development is influenced by or leads to left-right asymmetry in mammals. There is no doubt that developmental eye disease can result in asymmetrical phenotypes (Pasutto et al., 2007) and with a lack of evidence to the contrary we must assume that this asymmetry in humans is a result of either haplo-insufficiency coupled with genetic epistasis and/or environmental factors influencing one side rather more than the other. That said, if brain development is influenced by a separate organiser node (whose role is to determine left-right lateralisation) then a degree of separation of left eye development from right would be unsurprising.

# 3. Retinal symmetry

## *3.1. Neuroretina*

OCT is a non-invasive and non-contact tool for in vivo cross-sectional imaging of the internal retinal structure. Since its first description by Huang (Huang et al., 1991) multiple advances in the engineering of the light source and detector have brought new generations of the technology, with greater axial resolution and considerably faster scanning speed, resulting in higher-resolution images of the internal retinal morphology.

The introduction of spectral-domain OCT (SD-OCT), with its capacity for automated measures of retinal layer thicknesses, has aided the management of retinal diseases (e.g. diabetic macular oedema) that rely upon accurate information about changes in the retina (Forooghian et al., 2008). Importantly, there have also been studies of normal healthy eyes, partly to generate normative data (Realini et al., 2015), as much as to investigate how healthy eyes vary and change (Kelty et al., 2008). Studies have been performed in children (Altemir et al., 2013; Avery et al., 2015; Dereci et al., 2015; Huynh et al., 2007; A. Patel et al., 2016), young adults (Dalgliesh et al., 2015), and the older population (Grover et al., 2009), exploring the range of retinal measures from retinal nerve fibre layer (RNFL) thickness to macular volume. In addition, as well as cross-sectional measures, some attempt is being made to understand the natural history of normal ageing of the retina, and the early signs of sight-threatening pathology, as we seek to discover interventions that can alter this trajectory in susceptible individuals (Wessel et al., 2013).

### *3.1.1. Retinal thickness measures in health*

**Macular thickness:** Early studies of OCT-measured macular thickness in healthy eyes explored demographic associations and differences between racial groups. Wong and colleagues found that male gender, higher body mass index (BMI) and longer axial length were all associated with a significantly thicker central retina, in a study of 117 healthy subjects (Wong et al., 2005). However, they measured only right eyes and so did not comment on interocular symmetry. In addition, studies comparing racial groups have found thinner macula in African Americans compared with Caucasians (Asefzadeh et al., 2007; Kelty et al., 2008). These studies did compare left and right values, but found no significant asymmetry.

One study set out to specifically examine interocular symmetry of macular thickness and volume measurements, in a British population (n=100), and found no significant interocular differences in foveal thickness, or macular volume (El-Ashry et al., 2008).

However, all the above studies used the older and less precise time-domain OCT (TD-OCT) technology. There is an unfortunate paucity of large population-based studies of healthy individuals using the more precise SD-OCT – with its superior resolution - and little comment on interocular symmetry amongst those that have been published.

The Beaver Dam Eye Study was a large population-based observational cohort study of persons aged 43-86 years. 1544 of the participants received SD-OCT examination in 2008-2010, of which 977 were found to be healthy and free of retinal pathology (Myers et al., 2015). Unfortunately, no data on interocular symmetry from this dataset of healthy OCT scans has been published.

The largest resource of OCT data is the UK Biobank, a long-term cohort study following 500,000 volunteers aged between 40 and 69 years in the UK, of which 67,321 participants have had SD-OCT examination with the Topcon 3D-OCT (Topcon, Tokyo, Japan) (Keane et al., 2016). This is a tremendous resource, but again, in published reports of the macula thickness data, there are unfortunately no interocular comparisons (P. J. Patel et al., 2016).

**RNFL thickness:** In contrast to the lack of data on macular thickness, there is more data on the RNFL and its asymmetry.

The Sydney Childhood Eye Study in 2003-2004 used the Stratus TD-OCT (Carl Zeiss Meditec, Dublin, California) to measure RNFL thickness, in the macula and peripapillary region (Huynh et al., 2007). In their random cross-sectional sample of 1765 school-based children aged 6 years, they found a low level of interocular correlation of sector RNFL measures, with up to 17 μm difference between the eyes in average RNFL, and 47 μm difference in quadrants. There was no consistently thinner side, right or left, but the high level of asymmetry present was an important finding, and was later confirmed with SD-OCT in two studies in the paediatric population, one of 108 healthy children aged 6-17 years (Al-Haddad et al., 2014), the other in 357 children aged 6-13 years (Altemir et al., 2013).

In healthy adult studies, there is more consistent evidence that the RNFL is thicker in right eyes, even when adjusting for axial length, and excluding anisometropia (Dalgliesh et al., 2015; Yang et al., 2016). A large cross-sectional study of 617 healthy adults found significant interocular differences in all quadrants of the circumpapillary RNFL (cpRNFL) (Hwang et al., 2014).

These findings of a systematically thicker RNFL in the right eye (particularly temporally) were previously noted in studies of healthy subjects that used a scanning laser polarimeter, rather than OCT (Kurimoto et al., 2000). The importance of this finding of interocular asymmetry in RNFL is discussed further in Section 4.1.2. (glaucoma).

**GCL:** The ganglion cell layer and inner plexiform layer are often measured as a combined layer – known as the GC-IPL, or the ganglion cell complex (GCC) - as some SD-OCT machines cannot reliably discriminate the two layers. In contrast to the RNFL, the GC-IPL does demonstrate significant interocular symmetry, in studies of (n=275, n=158) healthy adults (Lee et al., 2015; Zhou et al., 2016).

**Outer retinal layers:** One particularly useful study from Cologne, Germany studied the symmetry of all retinal layers in 50 healthy individuals aged over 60 years, as a prelude to investigating the impact of silicon-oil endotamponade affecting those measurements (Caramoy et al., 2014). From their normal subject data, they reported moderate-to-high correlations between the eyes for retinal layer measures. although it is of note that RNFL and inner nuclear layer (INL) showed the lowest correlation coefficients, with the outer layer unification of posterior photoreceptor, RPE and Bruch's membrane next lowest in right-left concordance (Table 1). The weakness of the study is that it preceded the software upgrade on the Spectralis SD-OCT that enabled automatic segmentation of the individual layers. Therefore, the authors manually segmented the layers in image analysis software, before computing layer thicknesses. Nevertheless, it remains the only study to have attempted this interocular symmetry investigation of the full retinal layers.

**Table 1.** "Measurement repeatability, normative values and concordance of retinal layer volumes in eyes without macular pathology"

*Reproduced from:* 'Retinal layers measurements in healthy eyes and in eyes receiving silicone oil-based endotamponade', Albert Caramoy, Katharina M. Droege, Bernd Kirchhof, Sascha Fauser. Acta Ophthalmologica 2014; 92(4):e292-297. (Caramoy et al., 2014) Publisher: John Wiley and Sons. Reproduced unaltered under the terms of the Creative Commons Attribution Non-Commercial No Derivatives License CC BY-NC-ND.

| | **Measurement repeatability** | | **Retinal layer volumes ($mm^3$) Mean ± SD** | | | |
|---|---|---|---|---|---|---|
| **Variables** | **Right eye** | **Left eye** | **Right eye** | **Left eye** | **Concordance between right and left eyes** | **ICC CCC** |
| MACVOL | $r$ = 0.989<br>p < 0.001 | $r$ = 0.988<br>p < 0.001 | 3.101 ± 0.127 | 3.100 ± 0.136 | $r$ = 0.921<br>p < 0.001<br>$r_c$ = 0.919 | 0.992<br>0.984 |
| RNFL | $r$ = 0.905<br>p < 0.001 | $r$ = 0.931<br>p < 0.001 | 0.291 ± 0.023 | 0.291 ± 0.027 | $r$ = 0.734<br>p < 0.001<br>$r_c$ = 0.724 | 0.949<br>0.949 |
| GCLIPL | $r$ = 0.966<br>p < 0.001 | $r$ = 0.952<br>p < 0.001 | 0.745 ± 0.056 | 0.740 ± 0.060 | $r$ = 0.918<br>p < 0.001<br>$r_c$ = 0.913 | 0.975<br>0.942 |
| INL | $r$ = 0.808<br>p = 0.005 | $r$ = 0.649<br>p = 0.042 | 0.307 ± 0.025 | 0.313 ± 0.026 | $r$ = 0.759<br>p < 0.001<br>$r_c$ = 0.736 | 0.892<br>0.509 |
| Calculated inner retinal layers | $r$ = 0.914<br>p < 0.001 | $r$ = 0.846<br>p = 0.002 | 1.342 ± 0.081 | 1.344 ± 0.086 | $r$ = 0.901<br>p < 0.001<br>$r_c$ = 0.899 | 0.935<br>0.825 |
| OPLONLPIS | $r$ = 0.999<br>$r$ = 0.999 | $r$ = 0.996<br>$r$ = 0.996 | 1.102 ± 0.071 | 1.108 ± 0.070 | $r$ = 0.946<br>p < 0.001<br>$r_c$ = 0.942 | 0.999<br>0.994 |
| POSRPEBM | $r$ = 0.870<br>$r$ = 0.870 | $r$ = 0.930<br>$r$ = 0.930 | 0.644 ± 0.030 | 0.650 ± 0.029 | $r$ = 0.855<br>p < 0.001<br>$r_c$ = 0.841 | 0.914<br>0.856 |
| Calculated outer retinal layers | $r$ = 0.987<br>p < 0.001 | $r$ = 0.982<br>p < 0.001 | 1.747 ± 0.082 | 1.758 ± 0.078 | $r$ = 0.934<br>p < 0.001<br>$r_c$ = 0.924 | 0.989<br>0.978 |

$r$ = Pearson's product-moment correlation coefficient, $r_c$ = concordance correlation coefficient according to Lin. ICC = Intra class correlation coefficient for intra-examiner reproducibility, CCC = concordance correlation coefficient for interexaminer reproducibility, MACVOL = macular volume, RNFL = retinal nerve fibre layer, GCLIPL = ganglion cell layer and inner plexiform layer, INL = inner nuclear layer, OPLONLPIS = outer plexiform layer, Henle's fibre layer, outer nuclear layer and inner part of the photoreceptor layer, POSRPEBM = posterior part of the photoreceptor layer, retinal pigment epithelium and Bruch's membrane. Calculated Inner Retinal Layers = RNFL + GCLIPL + INL, Calculated Outer Retinal Layers = OPLONLPIS + POSRPEBM.

There are far fewer studies investigating the symmetry of outer retinal layers. In part, this is due to a limitation of OCT technology. The reflectance image produced by a SD-OCT machine is often misinterpreted as corresponding exactly to the anatomical neuronal layers. Whilst it is reasonably representative of the inner retina layers' thicknesses, the reflectance of the outer layers and more importantly the boundaries of those layers create reflectance lines on the OCT image that are far 'thicker' than the histological layer they are attributed to. Recognition of the importance of correct interpretation of the OCT image in the outer retina is reflected in recent updates on the nomenclature for these layers, for example the renaming of the inner-outer photoreceptor junction line as the ellipsoid zone (Staurenghi et al., 2014).

There are other imaging modalities that can be used to look the outer retinal layers. One study used a prototype adaptive optics retinal camera (rtx1: Imagine Eyes, France) to look at the parafoveal cone photoreceptors, in 20 healthy subjects (Lombardo et al., 2013). Despite finding a significant variation in cone density between subjects, there was a high level of interocular symmetry in each subject, with largely symmetrical cone densities at all locations measured (ICC $\geq 0.86$, $P < 0.001$).

**OCT machine normative databases:** Normative databases within the software of SD-OCT machines provide useful visual references of normality for individual patient scanning episodes. However, these normal databases have been incorporated with the assumption of complete retinal symmetry. For example, the Heidelberg Spectralis (Heidelberg Engineering, Heidelberg, Germany) device normative database for macular thickness is based upon a study of 201 healthy volunteers, where one eye was used and the machine now uses that same normative spread identically for each eye, (Grover et al., 2009)

Data on the normative database for the Spectralis SD-OCT nSite RNFL thickness protocol is not expressly published, but can be retrieved from the device by generating multiple varied-age hypothetical subjects on the device. This process reveals identical normal values for left and right eyes.

The same assumption of symmetry of all retinal layer thicknesses is seen on the normative data within the Cirrus SD-OCT (Carl Zeiss Meditec, Dublin, California) machine (Liu et al., 2011).

In summary, from the published data on interocular comparisons of retinal layer thicknesses using SD-OCT in healthy eyes, it appears there is indeed a degree of asymmetry, particularly in

the RNFL, in all age groups, and this appears systematic even when adjustments are made for refraction and biometry. In the past, we may have assumed interocular asymmetry within the retina was an abnormal sign, and in need of further investigation. But it is now clear that significant asymmetry of retinal layer thicknesses exists in health, throughout life, and this should be accounted for in both clinical and research settings. Much larger studies with adequate numbers of subjects at different age strata are required to provide reliable data on when asymmetry strays outside the bounds of normality in each region or layer of the retina.

### *3.1.2. Hereditary retinal disease*

Uniocular pigmentary retinopathy is usually caused by either inflammation or trauma. Unilateral retinitis pigmentosa (RP) has long been proposed (Dreisler, 1948) and case reports exist in the literature (Farrell, 2009; Joseph, 1951; Kolb and Galloway, 1964; Mehra, 1962; Spadea et al., 1998; Thakur and Puri, 2010; Weller et al., 2014). Indeed, the prevalence of unilateral disease has been reported to vary between 0.02 and 5% depending on the population studied (Gauvin et al., 2016) but its existence has been a controversial one. To confirm that the disease is truly inherited retinitis pigmentosa, a diagnostic electroretinogram is required and other, rarer causes of unilateral pigmentary retinopathy such as cancer-associated retinopathy and acute zonal occult outer retinopathy must also be ruled out (Francois and Verriest, 1952). Ideally, a mutation associated with RP must be proven.

Most of the isolated case reports and cohorts of unilateral RP have come without genetic diagnosis, but in recent years some evidence has emerged that it could be a genuine disease. Entirely unilateral RP has been documented in patients who have USH2A mutations (Marsiglia et al., 2012) and it has even been shown that unilateral disease can result from inheritance of germline mutations, as in the case of a member of a family with an RP1 mutation (Mukhopadhyay et al., 2011). The pathophysiology of disease can only be speculated upon.

Genetic disease can affect just one eye, as in the case of retinoblastoma. Similarly, it has been proposed that a somatic mutation in a progenitor cell during the development of the ‘unaffected’ retinal tissue could cause a mosaicism that confers protection on the ‘normal’ eye and ameliorate the effect of the disease-causing mutation. Alternatively, such a somatic mutation could accelerate retinal degeneration in an eye already compromised by a germline mutation. Thus, a form of ‘localised’ genetic epistasis could cause one eye to degenerate at an increased rate. The

discovery that RP in the 'healthy' eye has been shown to manifest 30 years after the diagnosis of unilateral RP supports this (Gauvin et al., 2016) and so we are no closer to determining if unilateral retinitis pigmentosa truly exists.

### *3.1.3. Age-related macular degeneration*

The commonest retinal pathology, and the leading cause of visual loss in age over 50 is age-related macular degeneration (ARMD). This is well-known clinically as a bilateral disease, and usually broadly symmetrical in phenotype, albeit often with non-concurrent development. The last decade has seen acceleration in our understanding of genetic susceptibility to ARMD, and also the epigenetic mechanisms that influence progression and severity (Gemenetzi and Lotery, 2014). We should therefore expect symmetry of disease; however, this is not always seen.

Mann and colleagues (Mann et al., 2011) examined colour fundus photographs from 1114 patients with early or late stage ARMD. In early stage disease, drusen were graded and counted, and a good level of symmetry was shown, with a mean difference in number of drusen of 0.2, although with a large variance. For later stage of ARMD, defined as the presence of choroidal neovascular membrane (CNV) or geographic atrophy (GA), there was much less symmetry, with only 61% demonstrating a symmetrical phenotypic classification. Obviously, this exceeds the expected level of symmetry if eyes were independently affected by the disease, however it does suggest some unknown factor influencing the progression of the disease, leading to asymmetry at a single time-point, and possibly even end-point.

Their findings with respect to symmetry of drusen in early ARMD align with earlier smaller studies (Barondes et al., 1990; Gass, 1972). For later-stage or neovascular ARMD, there is asymmetry in cross-sectional studies, but much of that may reflect non-concurrent development, so it is interesting to also look at end-point of disease for final phenotype. Here, we see a higher level of symmetry, in the type of CNV (Chang et al., 1995) and consequent macular scarring (Lavin et al., 1991) or atrophy (Bellmann et al., 2002). A retrospective review of the participants in the Beaver Dam Eye Study found that subjects who developed any type of ARMD had a very high level of interocular similarity in phenotype, with 51% within 1 severity grade, and 90% within 2 severity grades (Gangnon et al., 2015),

Therefore, for ARMD, there is asymmetry in timing of progression, but reasonable symmetry in eventual outcome in phenotype. This likely reflects the complex genetic/environmental interactions that contribute to this heterogenous disease.

### *3.1.3. Retinal detachment*

The Scottish Retinal Detachment Study prospectively recorded 1202 cases of rhegmatogenous retinal detachment (RRD) across Scotland, and found right eyes were more commonly affected than left (54.9% vs 43.4%; $p < 0.0001$) (Mitry et al., 2011). This could not be explained by myopic anisometropia, or any other risk factors for RRD. The authors query whether this was associated with ocular dominance in some way, but this remains unknown. A further retrospective study of laser retinopexies for treating retinal tears also found a higher number in right eyes (Mahroo et al., 2015).

### *3.2. Retinal vasculature morphometry*

The advent of digital retinal imaging with image processing and analysis techniques over the past two decades has enabled a thriving field of research, particularly around retinal vascular topology (Patton et al., 2006b). Much of the work is focused on identifying and classifying pathological changes, for example in stroke and diabetes, (Doubal et al., 2009; MacGillivray et al., 2014) however any such development of biomarkers requires a thorough understanding of healthy vasculature and its natural history. There has been an assumption that there is a high level of symmetry between our eyes with regards to the retinal vessel morphology, but there has been little direct examination of this assumption.

Setting reliable criteria by which to judge the symmetry of the retinal vasculature is challenging. We know that the overall shape of the retinal vasculature in the left and right eye is broadly symmetrical, but detailed properties of the vasculature much less so: that is the specific path and shape of individual vessels, the location of bifurcations and junctions, and the values of various morphometric indices commonly found in the literature of retinal biomarkers of non-ocular disease, such as tortuosity, branching angles and geometry, and vessel calibres (or widths).

Here we offer a computational viewpoint, based on our experience of developing the VAMPIRE suite of computer software for retinal image analysis (Pellegrini et al., 2014; Perez-Rovira et al., 2011; Trucco et al., 2015, 2013a). We identify issues that, in our view, play a crucial role in assessing reliably and meaningfully left-right eye symmetry, accompanied by an overview of relevant work.

#### *3.2.1. Retinal vascular biomarkers*

Quantitative analyses on left-right eye symmetry are mostly embedded in papers concentrating on other issues, typically the investigation of retinal biomarkers. The retina is unique in allowing easy, *in vivo* observation of a rich microvascular network simply and non-invasively. Confirming that morphometric properties of the retinal microvasculature are predictive of microvascular change in the brain and other organs, therefore contributing to early risk assessment, is a major area of research activity (MacGillivray et al., 2014). Indeed, detailed clinical observations of characteristic fundus features have led to the identification of early indicators of a range of non-ocular conditions such as stroke (Baker et al., 2008; Doubal et al., 2010), hypertension (Wong et al., 2007), cardiovascular disease (Liew and Wang, 2011), and of diabetic retinopathy (Cheung et

al., 2010). Also, retinal blood vessels may contribute to risk assessment for neurovascular diseases, as they are part of the brain's vascular system, thus sharing anatomical features and responding similarly to stress and disease (London et al., 2013; Patton et al., 2005).

### *3.2.2. Retinal vasculature software analysis*

VAMPIRE (Vessel Assessment and Measurement Platform for Images of the REtina) is an international initiative led by the Universities of Edinburgh and Dundee (Scotland, UK). The main software tool is interactive and allows operators to measure efficiently more than 100 morphometric parameters of the retinal vasculature per image, in large numbers of fundus camera images. Measurements include classic retinal biomarker candidates like summative measures of vessel calibre near the optic disc, estimates of vessel tortuosity, and the fractal dimension of the vascular network, computed by zone, quadrant and vascular tree. Figure 2 shows intermediate structures computed by the tool, namely the production of a binary map of the vessels, and the analysis of the arteriole and venule size and morphometry. Images are processed in batches and results saved in tabulated spreadsheets. Further VAMPIRE software tools enable a similar semi-automatic analysis of the retinal images produced by scanning laser ophthalmoscopes, such as Heidelberg Spectralis SLO (Cameron et al., 2016) and the ultra-widefield-of-view retinal images acquired by Optos SLO (Pellegrini et al., 2014).

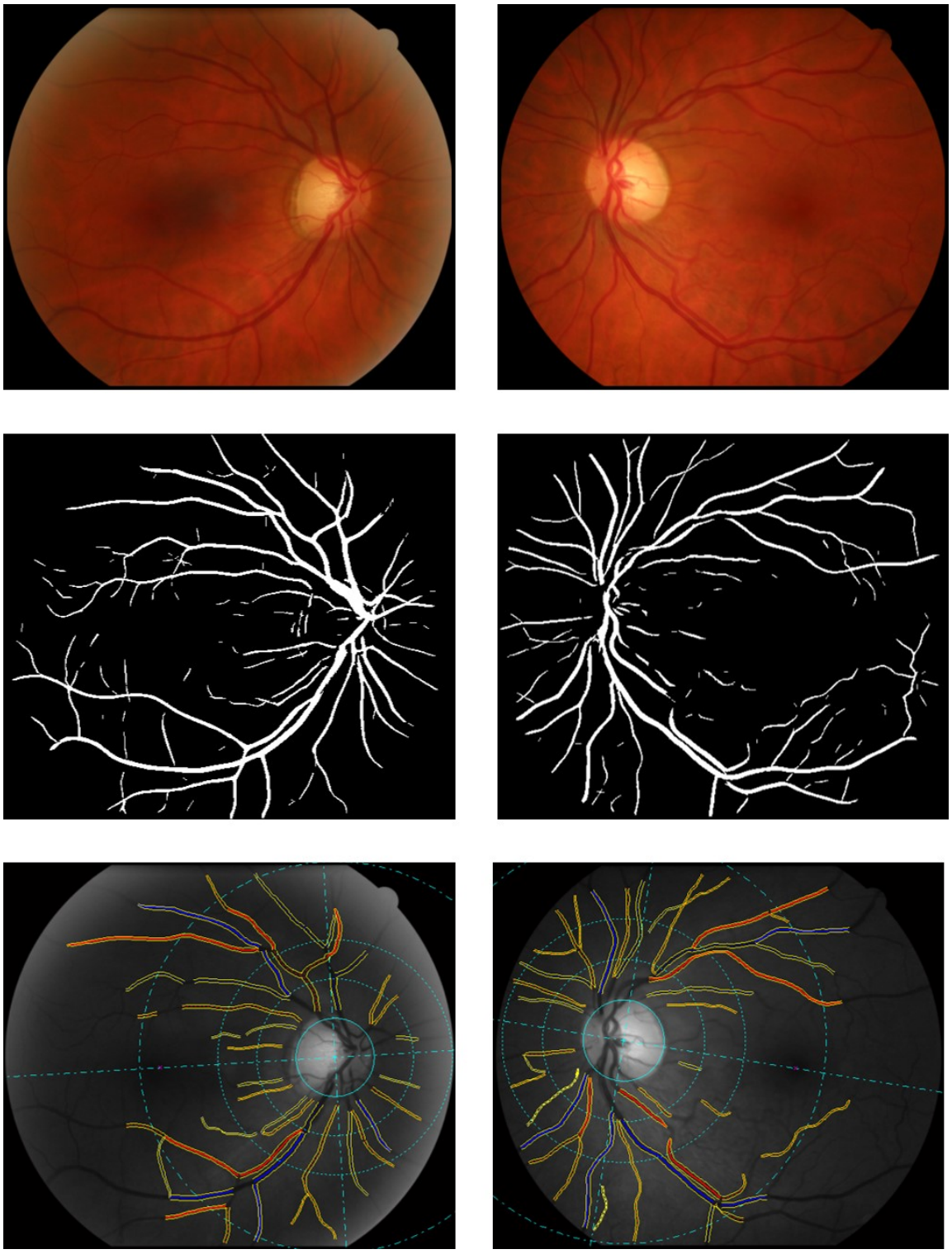

**Figure 2.** Computerised analysis of the retinal vasculature morphometry appearing in colour fundus imaging of the right and left eyes of an individual, using VAMPIRE. Image processing automatically detects retinal vessels in these fundus images to create binary maps where vessel pixels have been marked white and everything else remains black. Further processing classifies vessels as either arteries (red) or veins (blue), identifies the vessel boundaries (yellow) to compute width and measures additional properties such as vessel tortuosity, branching geometry and fractal dimension of the detected network pattern. Here, only a few arterioles and venules are labelled for illustration.

*3.2.3. Assessments of vessel symmetry*

High levels of correlation between retinal vessel diameters measured in right and left eye pairs have been reported in the Blue Mountains Eye Study, a large Australian population study, which examined 3,654 community-dwelling people aged over 49 years. Pearson correlation (*r*) was used in a random subsample (n = 1546) for summary indices of the width of retinal arterioles (CRAE, or central retinal arteriolar equivalent; $r = 0.70$), venules (CRVE, or central retinal venular equivalent; $r = 0.77$) and the arteriole-to-venule ratio (AVR, or arteriole-to-venule ratio; $r = 0.52$) (Leung et al., 2003). However, a Bland-Altman analysis revealed only a reasonable level of agreement, and that the mean arteriolar diameter was slightly but consistently larger (~2%) in the right eye compared to the left. The authors nevertheless concluded that measurements of retinal vessel diameter from one person's eye were adequate in representing the other eye, for the purposes of the paper's investigation.

Similar levels of correlation were reported in a sample of images (n = 838) from the Beaver Dam Eye Study (Wong et al., 2004). Similar *r* values were found to those in the Blue Mountains Eye Study for CRAE ($r = 0.71$), CVRE ($r = 0.74$) and AVR ($r = 0.49$). The authors also looked at the association of retinal arteriolar diameters and blood pressure and found it to be similarly strong using either eye. Their conclusion regarding the interchangeability of eyes for measuring vessel diameters was again one of adequacy. They did not further define "adequacy" in terms of sensitivity and reliability.

Using VAMPIRE, we have measured the fractal dimension of the retinal vascular network as a means of quantifying the branching pattern at it appears in fundus camera images in a community-dwelling cohort aged 73 years (n = 648) in the context of an investigation on retinal biomarkers for cognitive decline. We found only moderate correlations between left and right eyes ($r = 0.403 – 0.582$) (Taylor et al., 2015).

Other features of the retinal vasculature are also thought to reveal abnormalities or have the capacity to demonstrate deviation away from the optimal or healthy network arrangement, and may thus be indicative of disease. We have previously studied vessel tortuosity and branching geometry in the context of right and left eye asymmetry with data from the UK Biobank (MacGillivray et al., 2015). We accessed fundus camera images for a subset of participants (n=957). Using VAMPIRE software, 4 operators measured, per image, tortuosity for the 2 thickest arterioles and 2 thickest venules as well as branching geometry for 3–5 arteriolar and 3–5 venular bifurcations from locations detected automatically. The software calculated the median

for each set of measurements in order to summarise arteriolar and venular indices. Ocular bilateral agreement was assessed using intraclass correlation coefficient (ICC) (2-way mixed model) analysis. Single measure coefficients and 95% confidence intervals (CI) are reported. Spearman's correlation coefficient was also used to examine correspondence between right and left eye measurements. Statistical analyses were performed using SPSS software version 22.0 (SPSS Inc, Chicago, Illinois, USA). While positive but low correlations (<0.223) were present and significant (<0.05) for all variables, ICC agreement between retinal parameters measured in separate eyes was poor (<0.142) (Table 2). Bland-Altman analysis revealed average differences between right and left eyes close to zero for all measurements (Table 2). The greatest mean difference was between measurements of right and left arteriolar branching angle (mean difference=0.319°; 95% CI, 29.54 to -28.90). Figures 3 to 8 plot the absolute difference in measurements (left minus right eye) against the mean of left and right eye measurements. Examination of the Bland-Altman plots show that the difference in variance increases with higher values. Higher values demonstrate greater variance for all measurements, particularly log transformed tortuosity (Figures 7 and 8).

These findings do not provide support for the assumption of bilateral equivalence of retinal vascular branching and tortuosity measurements.

**Table 2.** Analysis of interocular symmetry from UK BioBank VAMPIRE study (MacGillivray et al., 2015)

| Vessel | VAMPIRE measure | N | Right | Left | | Bland Altman | Spearman's | |
|---|---|---|---|---|---|---|---|---|
| | | | Mean (SD) | Mean (SD) | ICC (95% CI) | Mean difference (95% limits of agreement) | Coefficient | P value |
| Arteriole | BA | 966 | 74.400 (11.205) | 74.719 (11.200) | .115 (.05-.18) | 0.319 (29.54 to -28.90) | 0.117 | 0.0003 |
| | BC | 964 | 1.234 (0.217) | 1.192 (0.192) | .036 (-.03-.10) | -0.042 (0.051 to -0.060) | 0.064 | 0.05 |
| | Tortuosity | 1085 | -6.796 (0.89) | -6.76 (0.92) | .141 (.08-.20) | -0.033 (2.30 to -2.36) | 0.223 | <0.0001 |
| Venule | BA | 1079 | 72.068 (9.241) | 72.122 (10.023) | .142 (.08-.20) | 0.054 (24.80 to -24.69) | 0.141 | <0.0001 |
| | BC | 1076 | 1.161 (0.13) | 1.14 (0.14) | .042 (-.02-.10) | -0.023 (0.34 to -0.39) | .064 | 0.036 |
| | Tortuosity | 1087 | -6.515 (1.04) | -6.57 (0.99) | .059 (.00-.12) | 0.051 (2.78 to -2.68) | 0.110 | <0.0001 |

*Note.* BA, branching angle; BC, branching coefficient; SD, standard deviation; ICC, intraclass correlation coefficient; CI, confidence interval. Tortuosity analyses conducted on transformed (natural log) data.

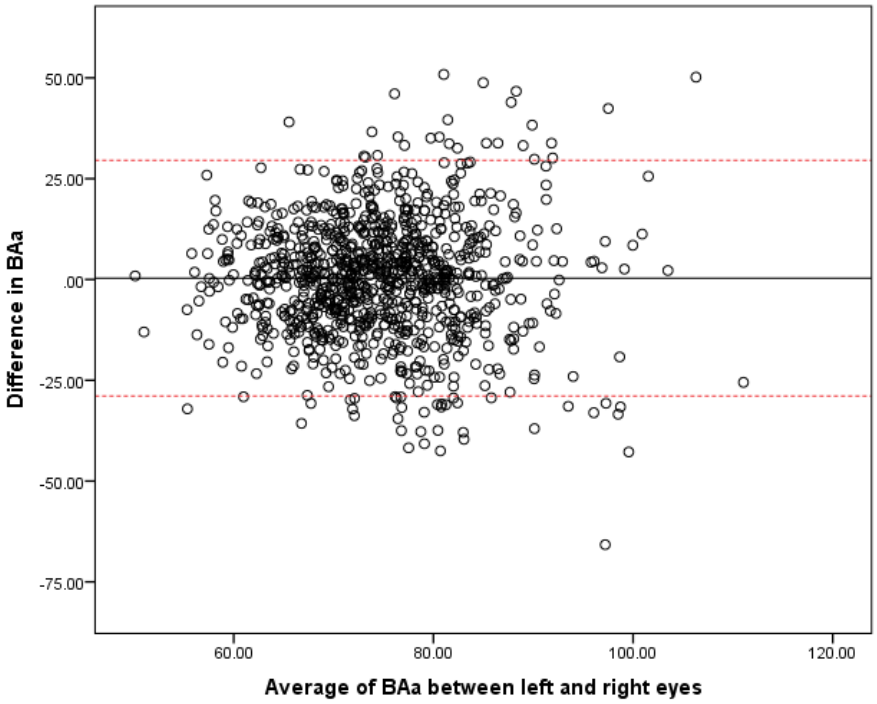


**Figure 3.** Bland-Altman plot of the difference in arteriolar branching angle (BAa, left eye minus right) against the mean of BAa of left and right eyes for UK Biobank sample (n=966)

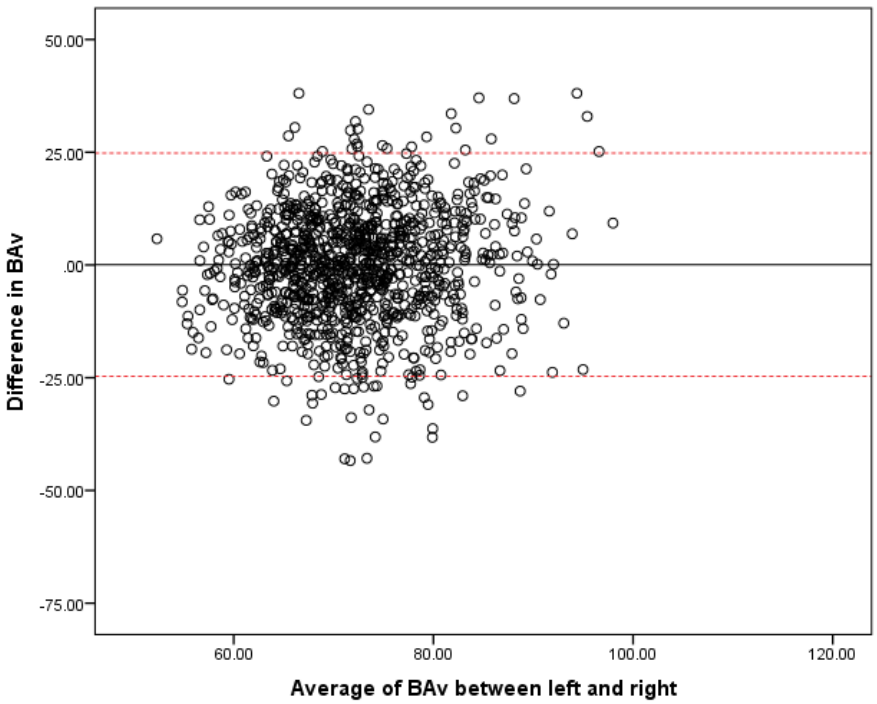


**Figure 4.** Bland-Altman plot of the difference in venular branching angle (BAv, left eye minus right) against the mean of BAv of left and right eyes for UK Biobank sample (n=1079)

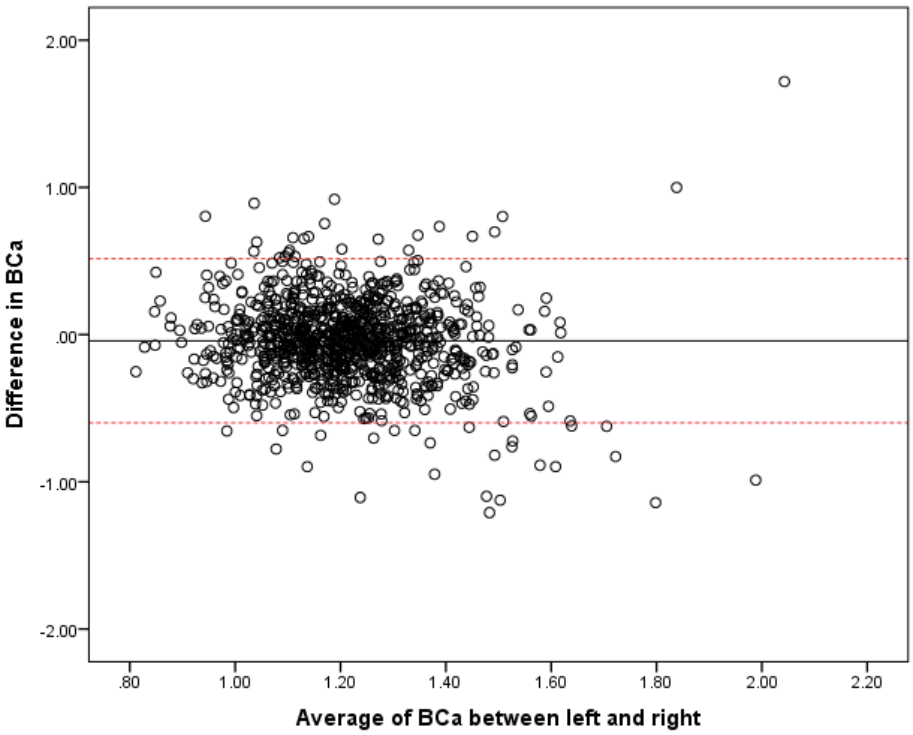


**Figure 5.** Bland-Altman plot of the difference in arteriolar branching coefficient (BCa, left eye minus right) against the mean of BCa of left and right eyes for UK Biobank sample (n=964)

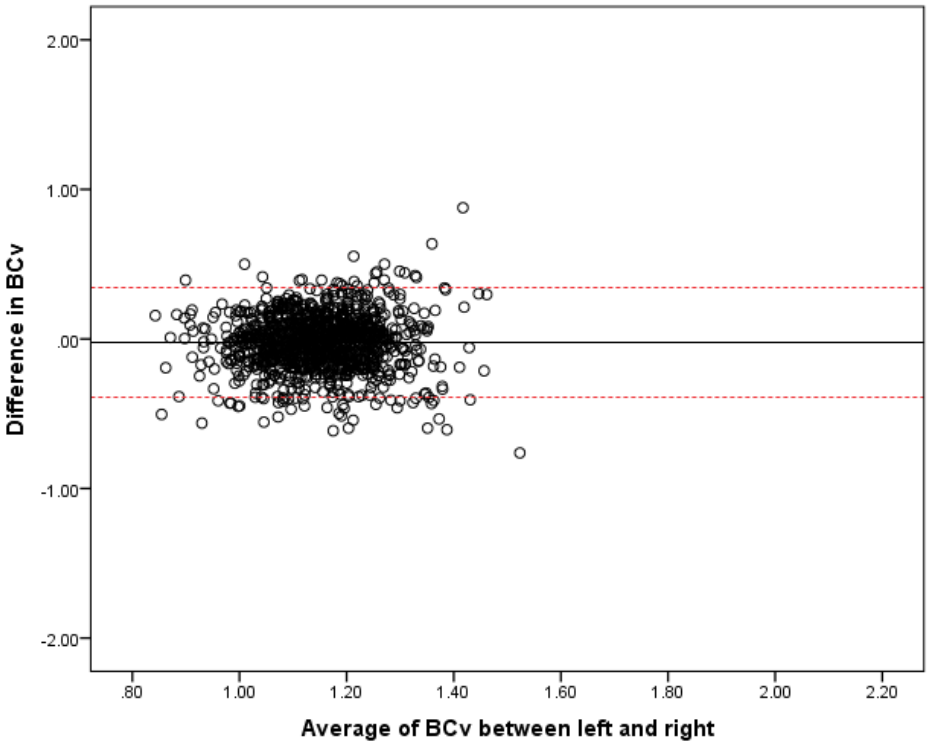


**Figure 6.** Bland-Altman plot of the difference in venular branching coefficient (BCv, left eye minus right) against the mean of BCv of left and right eyes for UK Biobank sample (n=1076)

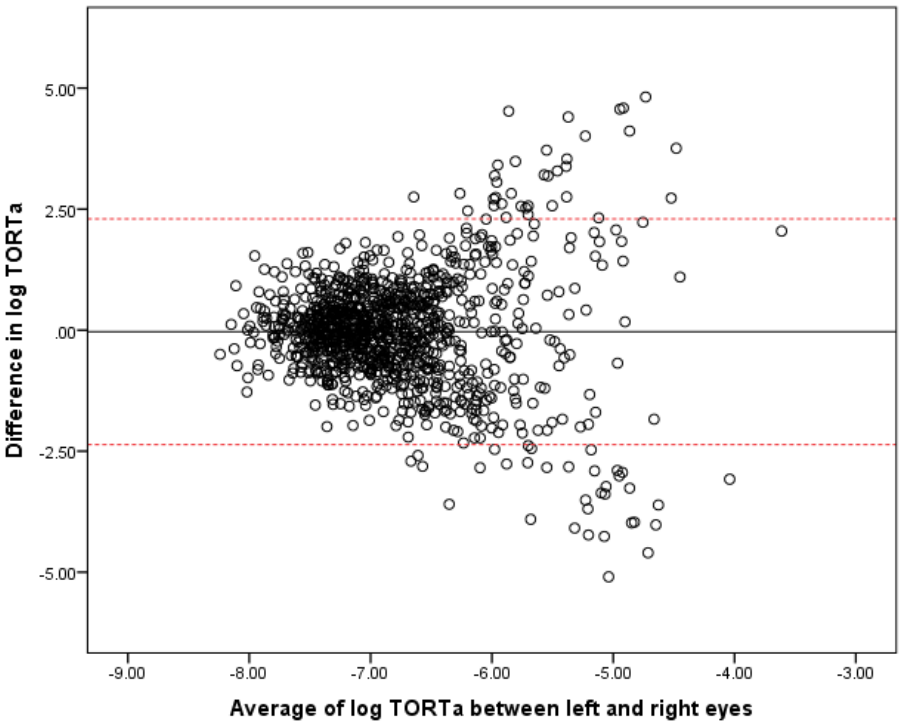


**Figure 7.** Bland-Altman plot of the difference in log transformed arteriolar tortuosity (log TORTa, left eye minus right) against the mean of log TORTa of left and right eyes for UK Biobank sample (n=1085)

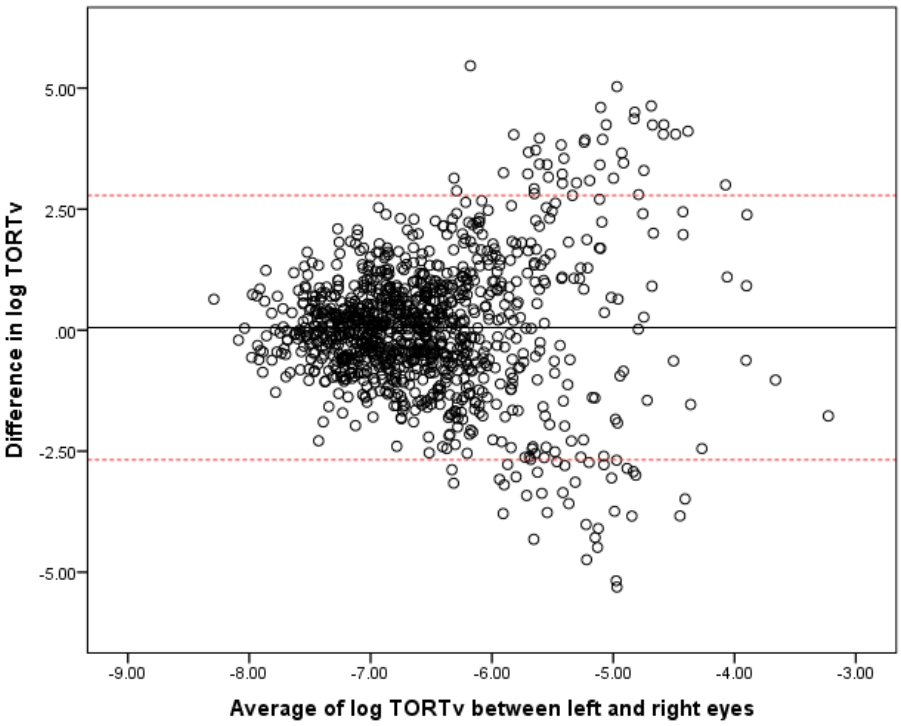


**Figure 8.** Bland-Altman plot of the difference in log transformed venular tortuosity (log TORTv, left eye minus right) against the mean of log TORTv of left and right eyes for UK Biobank sample (n=1087)

### *3.2.4. Which vessel parameters define symmetry?*

The level of symmetry between right and left retinal vascular morphology remains an open and complex question. If this symmetry must be assessed quantitatively, various definitions and choices must be established.

Firstly, the choice of direct or composite metrics of retinal vessels. Direct measurements are those measured directly on individual vessels, like vessel widths or tortuosity. Composite measurements, e.g. CRVE, CRAE and the ratio measurement AVR, are obtained from formulae combining direct measurements. Similar to large-scale properties, like the approximate shape and size of the main arcades (e.g. ellipse or parabola), they have the advantage of providing a summative assessment across the vasculature of one eye, but at the risk of potentially losing precision or sensitivity to small changes in a small number of retinal vessels.

Our work seems to indicate that different features may have different degrees of symmetry. Lower agreement between eyes is usually found for AVR, in comparison with CRAE and CRVE (Leung et al., 2003). This is of course expected, as errors introduced in the measurement of CRAE and CRVE would be amplified in the calculation of their ratios (Kronmal, 1993). Previous studies have reported slightly lower correlations for arteriolar widths than for venular widths (Couper et al., 2002; Leung et al., 2003; Wong et al., 2004). It was suggested that this is likely a reflection of the larger diameter of the retinal venules, but also the greater precision of measurement of venular width due to the greater contrast between the retinal background and the venule than for arterioles.

### *3.2.5. Choice of statistical measures of symmetry and agreement*

The choice of statistical tools to investigate left-right symmetry for a given measure and a given context (purpose and task) needs careful thought, as different indices reflect different types of association. For instance, Pearson correlation is a measure of *linear* dependence, and does not measure general agreement. A highly significant and large correlation coefficient can occur with gross bias (Bland and Altman, 1986; Ludbrook, 2002).

The ICC is a ratio of between-groups variance to total variance and reflects the degree of agreement between measurements. Results can be interpreted using the following criteria: 0.00 - 0.49 = poor, 0.50 - 0.74 = moderate, and 0.75 - 1.00 = excellent (Portney and Watkins, 2007). For some purposes, ICC will be sufficient. However, although ICC avoids the error of restricting

agreement to linear association for agreement, it is largely dependent on the range of values measured: the greater the variability between subjects, the higher the ICC value (Patton et al., 2006a).

Bland-Altman limits of agreement analysis has become increasingly popular method to examine agreement in clinical studies (Bland and Altman, 1986). Bland-Altman plots can be useful to illustrate the relationship between measurements from right and left eyes. This method involves calculating the difference for each pair of values and plotting these differences against the corresponding means for each pair. The values of the differences should be normally distributed and should be equally spread along all levels of the corresponding mean. The upper and lower limits of agreement (± 1.96 SD of the mean difference) reflect the boundaries within which 95% of the differences are expected to lie. Determining the level of agreement is a matter of clinical judgement. The plots can inform on the variability of agreement along the measurement scale, identify systematic bias or trend in the mean difference as well as extreme outliers (Patton et al., 2006a). Murray and Miller demonstrated the superiority of Bland Altman analysis over correlation in determining agreement (Murray and Miller, 1990).

### *3.2.6. Quantifying measurement uncertainty and error*

How should we quantify measurement uncertainty and its effect on statistical inference? Any measurement is subject to an uncertainty (limited accuracy) due to a number of factors, including image quality (MacGillivray et al., 2015), algorithm accuracy, image resolution, operator accuracy and repeatability for semi-automatic systems (Trucco et al., 2013b) to name only a few. The effects of such uncertainty on the reliability of statistical inference may have been underestimated. The situation is exacerbated in fully automatic systems, which do not try to limit uncertainty by operator corrections.

For instance, the reported accuracy of automatic artery-vein classification is around 90% (with specific data sets) (Dashtbozorg et al., 2014; Relan et al., 2013). What quantitative effect does a 10% error in vessel classification have on a statistical analysis taking the data at face value? It is possible that errors in measurement, artery-vein misclassification and image quality may distort the degree of asymmetry measured using computer-assisted techniques.

### *3.2.7. Linking vessel measures to known physiological outcomes*

Like other (but not all) measures, symmetry can be tested by *measurement*, i.e. comparing values of the same measurement (e.g. AVR) from the two eyes, or by *outcome*, i.e. comparing the results of associations with a given outcome (say the association with hypertension) using left and right-eye measurements independently. Both protocols have merits and are worth pursuing, ideally in parallel, although arguably the latter is the more important scientifically.

A truly comprehensive investigation should consider the variation of measurements in time, ideally over various time scales. It is known that vessel width, for instance, varies significantly within the pulse cycle, although there is no ultimate agreement about ranges (Hao et al., 2012; Knudtson et al., 2004) and no studies have used retinal fundus images that were gated to the cardiac cycle to increase consistency of measurement. It is also known that most retinal features change with age (Klein et al., 2000; Leung et al., 2003; Wong et al., 2003). Basing conclusions upon a single, random point in time seems to provide no more than an initial indication.

# 4. Brain and visual pathway symmetry

## *4.1. Optic nerve*

In this section, we look at optic nerve symmetry in health, and in the most common pathologies of the optic nerve: glaucoma, ischaemic neuropathy and optic neuritis, which all demonstrate varying degrees of laterality. We also compare these findings with the symmetry seen in hereditary optic neuropathies.

### *4.1.1. Optic nerve anatomy and normal ageing*

The optic nerve is around 6cm long, and is divided into 4 sections based on its path: intraocular, intraorbital, intracanalicular and intracranial (Wichmann and Müller-Forell, 2004). It is surrounded by meninges, and a subarachnoid space that is continuous with the corresponding intracranial subarachnoid space around the brain and spinal cord.

At a macroscopic level, our optic nerves are anatomically grossly symmetrical, in size and in course. Radiological scanning with computer tomography (CT) and magnetic resonance imaging (MRI), along with B-scan ultrasound of the intraorbital optic nerve, have all enabled measurements of the optic nerve and interocular comparisons to be made, in health, as well as in pathology; albeit to the limit of their resolution.

MRI studies of the optic nerve evolved in an early attempt to understand the pathophysiology of low-tension glaucoma (Stroman et al., 1995), and other optic neuropathies (Golnik et al., 1996). A comparison of MRI measures of optic nerve diameter in 23 living human subjects, with histology of 3 cadaveric specimens demonstrated a high level of agreement between the two, and also addressed interocular symmetry, finding no significant average interocular difference. (Karim et al., 2004). The same study confirmed that the diameter of the optic nerve gets thinner more posteriorly: 3.99 ± 0.04 mm anteriorly to 3.50 ± 0.04 mm posteriorly, reflecting reduced connective tissue within the nerve. There was no interocular difference throughout their length (Karim et al., 2004).

Optic nerve sheath diameter (ONSD) has become a more commonly studied measure, with computed tomography (CT) (Bekerman et al., 2016) or with B-scan ultrasound (Dubourg et al.,

2011; Newman et al., 2002) due to its clinical relevance of potentially providing a means of identifying or monitoring raised intracranial pressure.

A recent Turkish study of healthy population-based volunteers (n=198) used CT to measure the dimensions of the intraorbital optic nerve (Özer et al., 2016). They looked at the left-right symmetry and found no significant difference in optic nerve length. However, they did find a difference in ONSD, with right mean ONSD 5.53mm and left 5.61, p=0.009. When the whole study group was separated into male and female groups for separate analysis, this finding of a thicker mean left ONSD persisted in males, although it lost significance for the female group.

One study examined for differences between MRI and CT measures of ONSD (n=100) and found that the two modalities have very similar measures (Kalantari et al., 2013) at a threshold for discrimination of 0.2mm. Agreement between CT or MRI, and ultrasound, is less well-established, with one study reporting good agreement (Shirodkar et al., 2015) whilst another reports poor agreement (Giger-Tobler et al., 2015). Measurement of ONSD with ultrasound is clearly more convenient, but appears to be more variable. A study in healthy volunteers found symmetrical ONSD measurements at the resolution of the device (0.1-0.2mm) but high inter-operator variation of 0.6-0.7mm ($95^{th}$ centiles) (Ballantyne et al., 2002). With these unresolved issues of agreement and repeatability, we are unlikely to be able to make conclusions on optic nerve interocular symmetry at present.

More precise, microscopic measure of the optic nerve is feasible for the more accessible anterior intraocular section, with retinal imaging; and of course the primary component of the optic nerve – the retinal ganglion cells' axons - continues into the nerve fibre layer, which is now quickly and precisely measured with SD-OCT. Attention has been on attempting to understand the natural course of the optic nerve integrity through life, and the trajectory of normal ageing, by focussing studies on children and in the elderly. Through the published data in some of these studies, we can identify aspects relevant to our question of interocular symmetry.

A recently published study looked at the feasibility of using a handheld SD-OCT device in a range of children ages, from 1 day old to 13 years (n=352), to study optic nerve head development (A. Patel et al., 2016). Their focus was on the feasibility, quality and reliability of the imaging, and generation of some normative data for this population. However, they also reported the data and showed a high intraclass correlation coefficient (ICC) between the eyes for

measures of optic disc diameter (ICC=.892) and cup-to-disc ratio (ICC=.755). This symmetry continued as the discs slowly enlarged in size over the age groups of children being studied.

However, other studies have shown a greater degree of asymmetry in optic disc morphology in older children (Altemir et al., 2013; Huynh et al., 2007) particularly in measures of cpRNFL as discussed in Section 3.1.1. Altemir suggests setting the interocular difference in cup-to-disc ratio at a threshold of 0.25 before considering it pathological, reflecting the significant asymmetry in cup-to-disc ratios observed.

Macula and RNFL measurements change with normal ageing, with one study showing average RNFL thickness to decline by an average of -0.52 μm/year, with faster rates of decline in the superior and inferior sectors (-1.35 μm/year and -1.25 μm/year respectively) (Leung et al., 2012). This study however, included only 70 eyes of 35 subjects and had a relatively short follow-up time of 30 months. Similar rates of age-related decline in macular GC-IPL thickness have also been reported (Leung et al., 2013).

In a review of healthy elderly participants of the Blue Mountains Eye Study, they analysed the optic disc morphology in the 1276 healthy participants who had HRT3 (Heidelberg Retina Tomograph) scans of both eyes available (Li et al., 2013). They also found a high correlation between eyes in disc area, but poor correlations of cup depth, cup volume and RNFL thickness.

### *4.1.2. Glaucoma*

Glaucoma is a progressive optic neuropathy and common cause of irreversible blindness (Tatham et al., 2015). The major, and only modifiable, risk factor is raised intraocular pressure (IOP). Glaucoma is characterised by accelerated loss of retinal ganglion cells (RGCs) leading to thinning of RGC-related retinal layers, including the ganglion cell and inner plexiform layers (GC-IPL) and retinal nerve fibre layer (RNFL), and thinning of the neuroretinal rim leading to enlargement of the cup of the optic disc. These structural changes are associated with progressive loss of visual field.

Loss of visual field can be detected using automated perimetry, however many patients with glaucoma develop structural changes before a repeatable field defect becomes apparent (Kass et al., 2002). Glaucomatous changes to the optic nerve head can be detected with slit lamp biomicroscopy or using optical coherence tomography (OCT), which provides an objective, quantitative measure of glaucomatous damage, for example using measurements of

circumpapillary RNFL (cpRNFL) thickness. OCT can also be used to detect glaucomatous macular changes including decrease in total macular and macular GC-IPL thickness (Hood et al., 2013).

Although glaucoma is typically a bilateral disease, asymmetry is common, particularly in the early stages (Medeiros et al., 2005). For example, the Blue Mountains Eye Study found that of those with glaucomatous visual field loss, 50.5% had unilateral defects and 49.5% bilateral defects (Lee et al., 2003). In fact, it is the emergence of asymmetry between the eyes that alerts the ophthalmologist to the possibility of glaucoma. Interocular differences in IOP (Cartwright and Anderson, 1988; Levine et al., 2006; Williams et al., 2013), optic disc characteristics (Armaly, 1969; Ong et al., 1999), OCT measurements of cpRNFL and macular thickness (Gugleta et al., 1999; Sullivan-Mee et al., 2013), and visual field sensitivity (Greenfield et al., 2007; Levine et al., 2006) are all features that raise suspicion of glaucoma. Indeed an interocular difference in cup-disc ratio of more than 0.2 has long been quoted as a diagnostic criterion for glaucoma (Armaly, 1969).

The detection of interocular asymmetry in optic nerve or macula parameters has some possible diagnostic advantages over using isolated measures from one eye. For example, OCT normative databases are often used to classify cpRNFL thickness as normal, borderline or outside normal limits, however, normative databases consist of relatively few subjects, and these subjects have homogenous ocular and systemic characteristics (Realini et al., 2015) (Figure 9). Parameters such as cpRNFL thickness exhibit wide overlap between healthy subjects and those with early glaucoma and are influenced by patient-specific factors including age, gender and ethnicity, increasing the chances of patients with different characteristics to those included in the normative database being misclassified. As many of these factors are intrinsic to the individual and will not influence interocular asymmetry, using the fellow eye of the same individual for comparison may overcome some of these limitations (Sullivan-Mee et al., 2013). Eye-specific factors such as axial length, which also exhibit wide inter-individual variation, and influence structural measurements, are also likely to be similar between eyes and so have less influence on interocular asymmetry (Li et al., 2013). A patient's fellow eye could therefore serve as a useful comparative reference for the index eye.

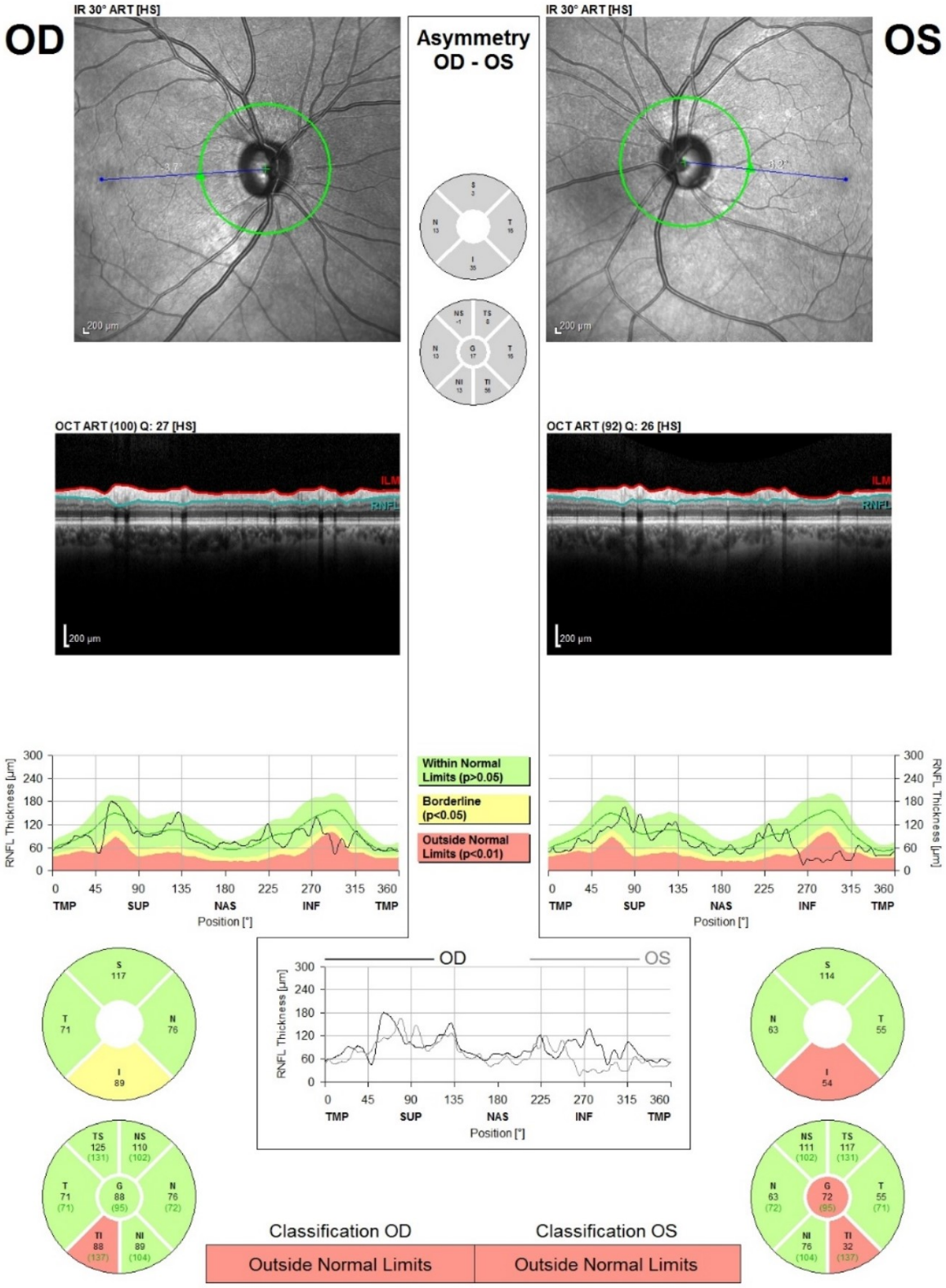


**Figure 9.** Optical coherence tomography circumpapillary retinal nerve fibre layer (cpRNFL) thickness analysis for a patient with glaucoma in both eyes (OD=right eye, OS=left eye) showing localised inferotemporal RNFL thinning in both eyes. Both eyes are classified outside normal limits with average RNFL thicknesses of 88µm in the right eye and 72µm in the left.

Several investigators have examined whether assessment of macular or optic nerve asymmetry is useful for discriminating between glaucomatous and healthy eyes and asymmetry analysis is now incorporated in commercial OCT software for glaucoma detection. The Blue Mountains Study, which also examined asymmetry in optic disc parameters in healthy compared to glaucomatous subjects found interocular asymmetry of vertical cup-disc ratio to be more common in those with glaucoma than healthy controls (Ong et al., 1999). 24% of those with glaucoma had cup-disc ratio asymmetry of ≥ 0.2 compared to only 6% of healthy subjects. 10% of those with glaucoma had cup-disc ratio asymmetry ≥ 0.3 compared to only 1% of healthy subjects. Therefore, although a large difference in cup-disc ratio was likely to indicate abnormality, relatively few patients with glaucoma had such a difference and asymmetry was present in some healthy individuals. The authors concluded that asymmetry in vertical cup-disc ratio alone is unlikely to beneficial as a tool for detecting glaucoma in a population. They did not report whether right or left eyes tended to have the larger cup-disc ratio.

OCT is a more sensitive and objective tool for detecting asymmetry in retinal and optic nerve structure, however, there are surprisingly few studies examining interocular differences in cpRNFL and macular thickness in glaucoma. In 2008, using older generation time-domain OCT, Budenz reported a study of 108 normal volunteers where cpRNFL thickness had been measured in both eyes (Budenz, 2008). The mean cpRNFL thickness was significantly thicker in right compared to left eyes, with an average thickness difference of 1.3 μm (95% confidence interval 0.4 μm to 2.2 μm, P=0.004), with 95% tolerance limits of -10.8 μm and +8.9 μm. This suggested that, in a normal individual, total cpRNFL thickness should not differ by more than 9 to 11 μm between eyes. The conclusion was that differences greater than 9 to 11 μm might represent early glaucoma (Budenz, 2008).

Subsequent studies have confirmed that healthy subjects have differences in cpRNFL thickness between right and left eyes, which are important when considering whether indices of asymmetry could be used for glaucoma detection. Using the spectral-domain Cirrus OCT, Dalgliesh and colleagues examined 1,500 healthy subjects aged 16 to 19 years (Dalgliesh et al., 2015). Similar to the findings of Budenz, right eyes had significantly thicker total cpRNFL than left eyes but the average difference was less at 0.3 μm (P=0.0074). The 2.5% to 97.5% limits of asymmetry were 9.3 μm. Dalgliesh and colleagues also performed macular imaging but there was no significant difference in average macular thickness between right and left eyes. The 2.5% to 97.5% limits of asymmetry was 8 μm for average macular thickness (Dalgliesh et al., 2015).

Others have reported similar findings, with the difference in total cpRNFL thickness between eyes maintained, even after accounting for differences in axial length and disc area, parameters known to affect cpRNFL thickness (Ha et al., 2002; Mwanza et al., 2011; Park et al., 2005). There do however appear to be regional differences, with right eyes found to have significantly thicker average, inferior, nasal and temporal, but not superior cpRNFL compared to left eyes (Mwanza et al., 2011), and these differences possibly depend on ocular dominance rather than being intrinsic to laterality (Choi et al., 2014). Asymmetry may also be related to other factors such as age and race. For example, the African Descent and Glaucoma Evaluation Study (ADAGES) found healthy subjects of African Descent had larger asymmetry in optic nerve parameters such as cup volume and rim volume, however the effect of race lost significance after adjusting for disc area (Moore et al., 2013).

Asymmetry analysis is now included in OCT software to aid glaucoma diagnosis, for example, the Spectralis SD-OCT has a "posterior pole asymmetry analysis" (PPAA) scanning protocol that acquires thickness measurements from the central 20 degrees of the posterior pole and compares them to the fellow eye (Asrani et al., 2011) (Figure 10). The device automatically segments Bruch's membrane and the internal limiting membrane and calculates the distance between. Thickness measurements are then displayed in an 8 x 8 (64 cell) colour-coded grid centred on the fovea, with each cell representing a 3 x 3 degree square area. The grid is positioned along the fovea-optic disc or fovea-Bruch's membrane opening (BMO) axis (Jacobsen et al., 2015). Software then performs an interocular analysis by comparing thickness measurements in each cell to corresponding regions of the fellow eye and an intraeye analysis by comparing superior and inferior hemifields in the same eye.

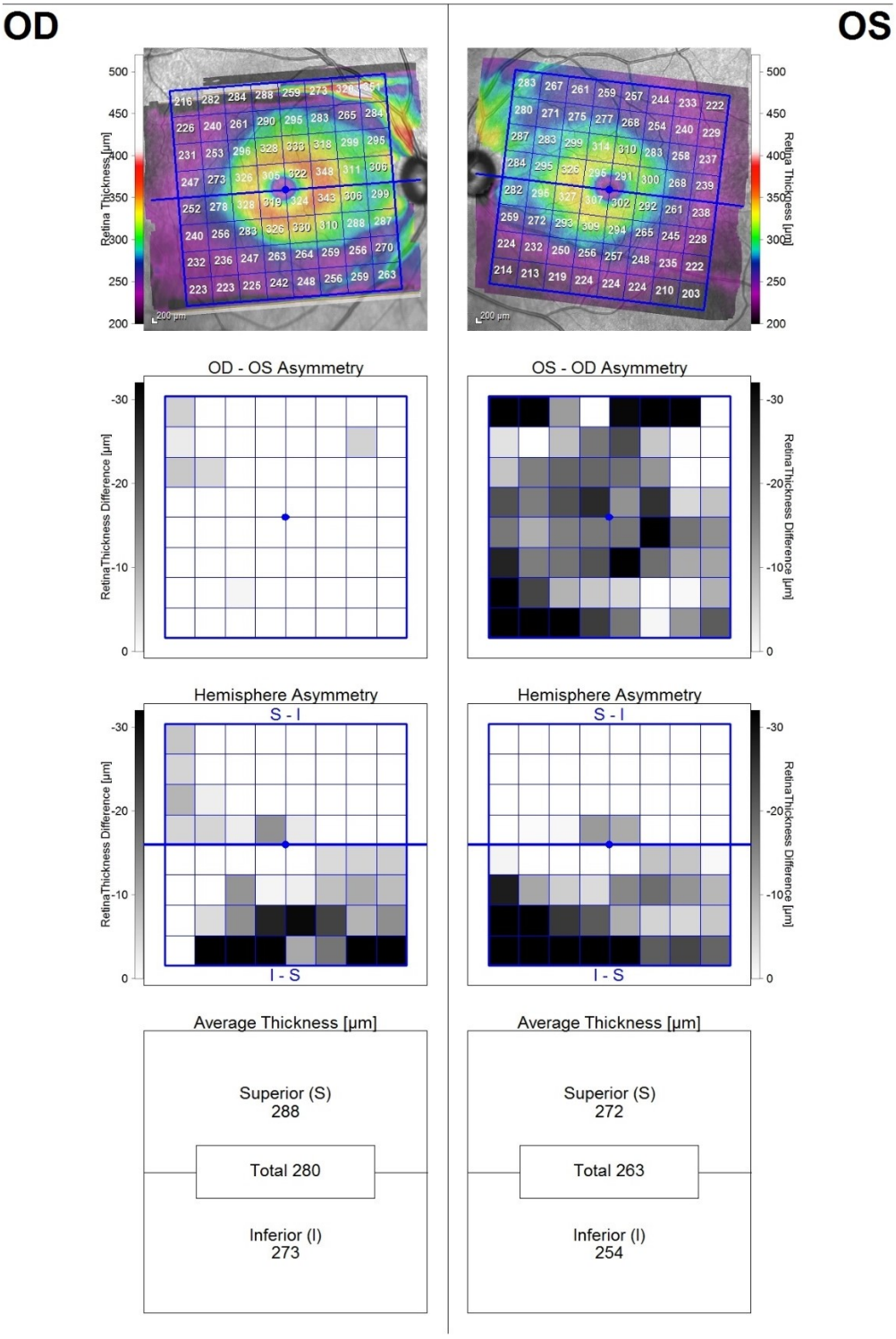


**Figure 10**. Optical coherence tomography posterior polar asymmetry analysis for the same patient as Figure 1. The majority of cells in the left-right eye (OS-OD) asymmetry plot are shaded greyscale indicating thinner retinal thickness in the left compared to right eye. In contrast, few of the cells in the left eye are thinner than the right (right-left (OD-OS) asymmetry plot). The hemisphere analysis indicates that the inferior retina in both eyes is thinner than the superior retina. The patient has a difference in macular thickness of 17 µm (280-263 µm), which is greater than the 5µm suggested as cut-off for detection of glaucoma by Sullivan-Mee and colleagues (Sullivan-Mee et al., 2013).

Sullivan-Mee and colleagues evaluated the ability of the PPAA-protocol to differentiate healthy and glaucomatous eyes (Sullivan-Mee et al., 2013). In a study of 100 eyes, including 50 with early perimetric glaucoma and 50 healthy controls interocular cpRNFL asymmetry had excellent ability to differentiate healthy and glaucomatous subjects with an area under the receiver operating characteristic curve (AUC) of 0.921, comparable with the best individual eye parameters (Sullivan-Mee et al., 2013). There was a wide range of normal cpRNFL values in healthy subjects (95% confidence interval of 80 to 116 μm), however variation in interocular difference in cpRNFL thickness was relatively small. Interocular difference in cpRNFL thickness was only 2.7 μm (95% CI 0 to 8.5 μm) in healthy subjects, compared to 14.6 μm (95% CI 2.5 to 33.0 μm) in those with glaucoma ($P < 0.001$). Using a diagnostic threshold value of 4.3 μm interocular difference in cpRNFL thickness achieved specificity of 82.4% for 80% sensitivity, and a cut off of 7.2 μm achieved specificity of 66% at 95% sensitivity. These results were similar to Field and colleagues who also found inter-eye asymmetry in cpRNFL thickness to be greater in those with glaucoma than controls (Field et al., 2016). An interocular difference in total cpRNFL thickness of 6.0 μm was determined the optimal cutoff value, achieving a sensitivity of 74% for specificity of 90% for differentiating normal and glaucomatous subjects.

Using the PPAA-protocol, Sullivan-Mee and colleagues also found interocular differences in macular thickness to have excellent diagnostic ability (Sullivan-Mee et al., 2013). Average macular thickness asymmetry was only 2.0 μm (95% CI 0 to 5.3 μm) in healthy subjects compared to 10.8 μm (95% CI 0 to 27.0 μm) in those with glaucoma. Interocular difference in macular thickness achieved an AUC of 0.913, with a cut off of 2.5 μm difference between eyes achieving 88.1% sensitivity for 80% specificity and a cut off of 4.2 μm achieving 82.5% sensitivity for 95% specificity. Coefficients of variation for interocular macular thickness, interocular cpRNFL thickness and total cpRNFL thickness were 0.46%, 2.81% and 10.2% respectively, indicating interocular cpRNFL thickness asymmetry to have 6.1 times greater variability than macular thickness asymmetry and total cpRNFL thickness to have a 22.2 times greater variability than interocular macular thickness. The mean interocular difference in cpRNFL thickness (14.6 μm) in glaucoma patients was 2 times higher than the suggested cut off value for detecting abnormality (7.2 μm), further indicating the possible value of cpRNFL asymmetry as a diagnostic tool. However macular thickness asymmetry performed even better, with an average value in glaucoma patients (10.8 μm) 2.5 times greater than the suggested cut-off

of 4.2 μm. The authors suggested that an interocular macular thickness asymmetry of 5 μm or more, or an interocular cpRNFL thickness asymmetry of 9 μm could be useful cut offs to indicate glaucoma (Sullivan-Mee et al., 2013).[11]

It is important to note, however, that 70% of patients with glaucoma included in this study had visual field loss in only one eye. One would expect measures of asymmetry to perform more poorly in patients with a similar degree of damage to right and left eyes and for performance to vary at different stages of disease. In advanced glaucoma, the cpRNFL and macular become too thin for OCT to detect further change, a phenomenon known as the floor in structural measures (Tatham et al., 2015). Performance of asymmetry indices is therefore likely to be worse in advanced disease, however in advanced disease, the diagnosis of glaucoma is usually straightforward without recourse to imaging or asymmetry analyses. Detection of early glaucoma is more challenging and in equivocal cases, recognition of asymmetric structural change may prove a useful aid to diagnosis, albeit, used in parallel with raw measurements from each eye.

A further limitation of current asymmetry metrics is the lack of a database of ranges of interocular asymmetry in healthy subjects that could inform decision-making regarding likelihood of disease. Jacobsen and colleagues have gone some way to addressing this problem by using the PPAA-protocol to obtain normal values for asymmetry in 105 healthy subjects aged 18 to 45 years (Jacobsen et al., 2015). The average interocular macular thickness asymmetry was only 5.6 μm (95% CI 4.6 to 6.5 μm) suggesting macular thickness to be remarkably symmetrical between right and left eyes of healthy subjects, similar to the findings of Sullivan-Mee and colleagues (Sullivan-Mee et al., 2013). However, asymmetry increased with age (0.04 μm per year, 95% CI: 0.02-0.06 μm) and was greater in men compared to women so these factors may need to be taken into account when determining if asymmetry is normal or not. The greatest asymmetry was in the superior and inferior nasal cells, probably due to the location of the vascular arcades in this region, which are included in the segmentation by the Spectralis OCT software. Further research into the relationship between ocular dominance and retinal thickness may also necessitate modifications to current OCT normative databases, for example, if dominant eyes are found to have a thicker cpRNFL than non-dominant eyes, the normal cpRNFL ranges may need to be adjusted depending on which eye is imaged.

It is also important to highlight the potential value of measuring intraeye asymmetry, or the difference in structural or functional characteristics between superior and inferior hemifields of the same eye. This is a potentially attractive option given that in healthy subjects the distribution

of RGCs is almost symmetrical between the superior and inferior halves of the retina (Curcio and Allen, 1990). Interestingly, one measure of intraeye asymmetry, the glaucoma hemifield test (GHT) has been used in automated perimetry for almost 25 years (Asman and Heijl, 1992). The GHT compares the intraeye visual field sensitivity in superior and inferior hemifields to determine whether an eye is within, borderline or outside normal limits. Intraeye asymmetry in retinal thickness is also evaluated in the PPAA-protocol of the Spectralis OCT.

Asymmetric loss of RGCs in glaucoma can also be detected using tests of visual function such as perimetry or pupillometry. Recently several investigators have examined whether detection of asymmetry in the pupillary light reflex might be useful for glaucoma detection (Chang et al., 2013; Gracitelli et al., 2016; Tatham et al., 2014). A recent review article found 30 studies examining the ability of a relative afferent pupillary defect (RAPD) to differentiate glaucomatous and healthy eyes, however the pooled sensitivity was only 63% (Chang et al., 2013). The pooled specificity was 93% however many other conditions can cause a RAPD and although the presence of a RAPD is likely to indicate an abnormality, asymmetry in pupillary light reflex is unlikely to have good discriminatory value.

Given that in healthy subjects cpRNFL thickness seems to be greater in right compared to left eyes, it is also interesting to consider whether glaucoma might preferentially affect one side. There is very little research examining laterality in glaucoma. A recent pilot study, which examined sleep position in glaucoma patients, did report lower cpRNFL thickness and worse visual field sensitivity in the left eye, which seemed to correlate to increased time sleeping on the right hand side (Kaplowitz et al., 2015). It is possible that sleep position might influence ocular perfusion, with decreased perfusion a possible risk factor for glaucoma. Sleep laboratory studies have also shown patients with glaucoma tend to have greater asymmetry in intraocular pressure fluctuation than controls (Liu and Weinreb, 2014).

### *4.1.3. Optic neuritis*

Optic neuritis describes an inflammation of the optic nerve, and is a term usually used in the swelling and demyelination seen in multiple sclerosis (MS)-associated optic nerve inflammation – the commonest cause of inflammatory optic neuropathy. Symptoms are usually unilateral although imaging and other tests may show bilateral involvement,

Few papers on unilateral optic neuritis report the affected side. The optic neuritis treatment trial (ONTT) did report this information in their second publication (Optic Neuritis Study Group., 1991). Of the 448 patients enrolled in the ONTT study, the right eye was affected in 49.6% of cases. No further comment was made on this, or any association between side and outcome, or between side and brain abnormalities on MRI. 49.6% does not represent a significant difference between left and right, from this sample size, with a one-sided t-test.

Nevertheless, the importance of optic neuritis and vision in understanding the pathway and progression of multiple sclerosis is increasingly recognised (Balcer et al., 2015). OCT measurement of RGC loss is now an agreed marker for clinical monitoring of MS, as well as an outcome measure in investigative trials (Saidha et al., 2015). Through increased use of OCT in MS trials, and correlation with brain changes, questions regarding symmetry or asymmetry in the disease pathophysiology and its presentation will be answered.

This ability to precisely (and easily) measure small changes in neuroretinal thickness, has led to a surge in research activity investigating the feasibility of such measures being surrogate markers of central brain white matter neural integrity in other neurological diseases such as Alzheimer's dementia (Cameron and Tatham, 2016; Thomson et al., 2015). The presence and relevance of symmetry within these measures is likely to emerge in coming years.

### *4.1.4. Hereditary optic neuropathies*

Hereditary optic neuropathies are generally considered as bilateral symmetrical diseases. Symmetrical in anatomical appearance, as well as in their functional impact upon vision. Advances in molecular understanding of their development, particularly with regards to mitochondrial dysfunction, have enabled better understanding of their pathophysiology and their broader phenotypic spectrum, benefitted diagnosis and counselling, and created potential for treatment strategies (Yu-Wai-Man et al., 2011).

Leber hereditary optic neuropathy (LHON) is a relatively acute and severe loss of central vision, occurring in young adults. The presence of optic nerve head swelling at acute presentation is a known finding, and the new technology of OCT-angiography has also revealed circumpapillary microangiopathy and dilated tortuous retinal vessels are present (De Rojas et al., 2016).

The typical presentation of LHON is of bilateral sequential optic nerve involvement, with the second eye affected usually within a few months. This does vary widely however, and it is the asymmetry in timing of onset of the disease that has led to speculation on possible environmental factors (Kirkman et al., 2009). In fact, one case is reported of an 18-year interval between eye involvement (Ohden et al., 2016). Unilateral cases are very rare, but have been reported (Nikoskelainen et al., 1996; Sugisaka et al., 2007).

This asymmetry, along with variability in the clinical expression of the disease, and the marked incomplete penetrance, mean there is much still to learn about LHON. The precipitant or trigger for the optic nerve dysfunction is still unknown, and the asymmetry in symptom onset may reflect an asymmetry between the mitochondrial reserve or resilience between left and right optic nerves.

Autosomal-dominant optic atrophy (DOA) has a similar prevalence to LHON but has a more gradual onset, and progression, and with a higher penetrance than LHON (Yu-Wai-Man et al., 2010). Whilst there is wide phenotypic variability, it carries a slightly better visual prognosis than LHON, although again no treatments are currently available.

Clinically, the presentation is more symmetrical in timing than LHON, and an OCT study of 16 patients with DOA measured RNFL thinning in both eyes, and found them “highly symmetrical”, although did not quantify this (Kim and Hwang, 2007).

Congenital optic disc abnormalities such as disc coloboma and megalopapilla are rare but also appear to demonstrate laterality.

Megalopapilla describes a congenitally enlarged (area > 2.5mm$^2$), but functionally normal optic disc (Brodsky, 1994; Franceschetti and Bock, 1950). It can be divided into two types: Type 1 is bilateral, and the more common Type 2 is unilateral (Randhawa et al., 2007). Patients are asymptomatic, with normal vision, visual fields, and normal rim volume when assessed with HRT3 (Sampaolesi and Sampaolesi, 2001). It is not associated with thicker optic nerves however, but has been described in association with contralateral optic nerve hypoplasia (Ahuja

and Traboulsi, 2010). It is not associated with glaucoma or any progressive change, and the cause of the abnormality is unknown, although a small genetically isolated population in the Marshall Islands was found to have a relatively high incidence of the finding (Maisel et al., 1989).

Optic disc coloboma is a deep excavation of the inferior disc, sometimes with absence of the adjacent area of retina and choroid, and with a wide range of syndromic associations (Dutton, 2004). Occurring as result of incomplete fusion of the two sides of the optic cup, PAX2 gene mutations have been thought responsible, possibly via impaired astrocyte differentiation (Chu et al., 2001). However, with equal incidence of unilateral coloboma as with bilateral, a more complex interaction of transcription factors during ocular morphogenesis is likely, perhaps with SoxC factors such as sox4 which is known for altering proximo-distal patterning of the optic vesicle in a zebrafish model of eye development (Wen et al., 2015).

### *4.2. Optic radiation, thalamus and visual cortex*

In this section, we will first consider the normal neuroanatomy of the visual pathways before describing neuroanatomical and functional lateralisation and asymmetry of the visual pathways in the healthy brain. We will then review asymmetry in the diseased brain concentrating first on cerebrovascular disease and then on other brain diseases with respect to the visual pathways. It is beyond the scope of this article to describe the well documented structural and functional asymmetries in other areas of the brain.

Of note, when considering the brain, despite obvious and long recognised asymmetries between the cerebral hemispheres being the norm, many computational image analysis programs and approaches assume that the brain is symmetrical and rely on intrinsic built-in steps that warp the brain of interest (i.e. that is being analysed) to a 'standard space' that makes the brain appear far more symmetrical than it actually is (Dickie et al., 2015). These steps can also change the size of individual structures relative to others, particularly small structures (Valdés Hernández et al., 2015). For this reason, we prefer to perform computational brain image analysis using 'native space' (i.e. described simplistically, the original brain stays in its original form) and registration and computational algorithms that preserve the original size and shape of the brain being processed (Wardlaw et al., 2011). Such approaches are likely to yield far more biologically reliable results, particularly when relating aspects of brain structure to other variables outside the brain, than those analysis approaches that change the fundamental shape and size of the brain to make it fit into a framework for the convenience of the computer program.

#### *4.2.1. Visual pathway symmetry in the healthy brain*

In considering symmetry in the visual pathways distal to the optic chiasm it is useful to first review the neuroanatomy. After the optic chiasm, nerve fibres connect to the thalamus, predominantly the lateral geniculate nucleus (LGN), which has 6 distinct layers which receive information from both the ipsi- and contra-lateral eye. It is felt that the LGN has a role to play in retinotopic mapping to the occipital cortex and that the pulvinar nuclei is concerned with attention when there are competing visual stimuli and may connect to the parietal lobe and the visual cortex (Kastner et al., 2004). From the LGN, projections proceed through the optic radiation to the left or right occipital lobes V1 region, and from there to V2 (Usrey and Alitto, 2015).

**Thalamus – lateral geniculate nucleus:** When examining the parts of the thalamus that deal with the visual pathways there are few data to suggest that the thalamus demonstrates clear structural asymmetry in the case of the lateral geniculate nucleus. Functional mapping of the human LGN with BOLD-MRI shows that both left and right LGN project symmetrically to the primary visual cortex with flickering stimuli in the left and right visual hemifields (Kastner et al., 2004). There is some evidence however that the medial geniculate nucleus (which plays a key role with connections to the primary auditory cortex) in the thalamus demonstrates asymmetry (Eidelberg and Galaburda, 1982) and this was postulated to reflect lateralisation of speech function to the dominant hemisphere.

**Thalamus – pulvinar nuclei:** The pulvinar nuclei predominantly receive afferent projections from the visual cortex and often display bilateral hemifield sensitivity. There are no obvious structural differences between the left and right pulvinar nuclei, however functional imaging with BOLD-MRI suggests that during certain tasks related to attention and in particular concerning the shift of visual attention the left pulvinar might exhibit more activation that the right pulvinar nucleus (Cotton and Smith, 2007) and that this may correlate with left parietal lobe activation during this shift of attention (Yantis et al., 2002). We should stress however that the functional organisation of the pulvinar nuclei (in contrast to primate knowledge) is not yet fully understood.

**Optic radiation:** In keeping with the thalamus there is no clear evidence of asymmetry in the optic radiations leading from the thalamus to the occipital cortex, except differences in length or distribution required to match asymmetries in the occipital lobes which are common.

**Occipital cortex:** In contrast to the other areas of the post chiasmal visual pathways there is clear evidence of asymmetry between left and right in the occipital cortex (perhaps reflecting a difference in embryological development or disease but also that the occipital cortex is a larger part of the brain and easier to measure). Petalias (asymmetrical protrusion of one part of the cerebral cortex compared with the other side, named initially after the indentations seen in the skull base) have been described in the frontal and left occipital cortex on CT (Le May and Kido, 1978), early MRI (Kertesz et al., 1986) and confirmed in voxel based morphological MRI analysis (Watkins et al., 2001).

Perhaps unsurprisingly given the clear structural asymmetry demonstrated in the occipital lobes there is emerging evidence that there is asymmetry evident in the functional anatomy of these areas. BOLD analysis to visual stimuli demonstrates that there is a general lateralisation of cerebral activity towards the right hemisphere for early visual cortex areas and for areas involved

with higher level visual processing (e.g. attention) – corrected for other factors and only partly explained by an increased grey matter volume in these areas (Hougaard et al., 2015) and this laterality shifted to the left with increasing age. This bias may explain the phenomenon of left field preference in some visual perception tasks (Verleger et al., 2009). Fascinatingly, right cortical electrical stimulations were more likely that left cortical stimulations to produce visual hallucinations in patients with epilepsy (Jonas et al., 2014). Further demonstrating the lateralisation present in many higher visual centres, the processing of symmetry perception appears to produce more activity in the right posterior regions (Bertamini and Makin, 2014), and colour discrimination is also processed in the right cerebral hemisphere (Danilova and Mollon, 2009).

### *4.2.2. Cerebrovascular disease impacting the visual pathway*

The brain is supplied by the two carotid and two vertebral arteries. While the internal carotid arteries are generally of similar size and flow velocity, the vertebral arteries are commonly asymmetrical. The Circle of Willis, through which the two internal carotid and basilar arteries (via the posterior cerebral arteries) anastomose, is commonly incomplete and asymmetrical. Thus, internal carotid artery asymmetry of flow velocity or diameter during a radiological examination would trigger a hunt for a reason (Lewis and Wardlaw, 2002), whereas vertebral asymmetry is the norm and in fact can create difficulties in assessing whether the flow on one side might be pathological in the presence of posterior circulation symptoms. Given that the vertebral arteries usually join together to form the basilar artery which then supplies most of the posterior fossa, asymmetrical disease in the vertebral arteries does not usually lead to asymmetrical disease in the posterior cerebral arteries.

Studies of stroke report a higher proportion of patients with left sided stroke than right (56% versus 44% in a large German series, n >11000) (Foerch et al., 2005) but, while there are a few pathophysiological reasons for this to occur, it is more likely that this represents the lateralisation of higher cerebral functions (in particular neglect and speech) so that right brain strokes which do not tend to cause speech disturbance are less likely to be recognised by the individual or others and hence under reported and under recognized (Hedna et al., 2013). This theory was supported by evidence from the Rotterdam population based study demonstrating that there were more incident left than right hemisphere strokes reported but equal prevalence of left and right cerebral hemisphere infarcts on magnetic resonance imaging (Portegies et al., 2015).

Theoretical reasons why cardiac emboli may be more likely to pass up the right than the left common carotid arteries (cardioembolic sources accounting for about a quarter of ischaemic strokes) include that the origin of the right CCA is located more directly above the aortic origin than is the left CCA. Therefore the presence of any asymmetry should not be surprising. Additionally, the distribution of infarcts in a study depends on patients surviving for long enough to get into the study; differences in survival between right and left hemisphere strokes may influence perceived laterality (Sposato et al., 2016).

All forms of 'silent' cerebrovascular disease that have been studied to date tend to result in symmetrical distribution of lesions in the brain including white matter hyperintensities (WMH), lacunes (Valdés Hernández et al., 2015), microbleeds, and secondary features such as perivascular space prominence and cerebral atrophy (Wardlaw et al., 2013). While the symmetry may not be perfect, in general these features of microvascular disease appear in both cerebral hemispheres and on both sides of the brainstem and progress fairly evenly on both sides, even when there is evidence of grossly asymmetric disease such as a tight atheromatous stenosis in one of the proximal internal carotid arteries but not the other (Potter et al., 2012; Wardlaw et al., 2014). Indeed the symmetry of features such as WMH is such that in some situations (e.g. where a discrete infarct in the contralateral hemisphere makes differentiation of the WMH difficult for image processing) it is reasonable to assess one hemisphere only and double it as a proxy for disease load in the whole brain (Valdés Hernández et al., 2016).

None of the factors influencing symmetry in the neck or large intracranial arteries have been taken into consideration in any studies of retinal vascular geometry to date, nor have there been comparisons of symmetry of retinal features and distribution of cerebral small vessel lesions.

### *4.2.3. Other brain disease*

There are minimal data on symmetry of the effect upon the visual pathways in other brain diseases. There is however some accumulating evidence that brain parenchymal asymmetry may influence or be associated with other cognitive disorders including dementia (Cherbuin et al., 2010; Derflinger et al., 2011). In patients with dementia there is symmetrical left/right reactivity in the posterior cerebral arteries (PCA) using light stimulation and transcranial Doppler ultrasonography (TCD) (Asil and Uzuner, 2005).

Demonstrating clear lateralisation of higher visual functions, right cortical electrical stimulations were more likely than left cortical stimulations to produce visual hallucinations in patients with epilepsy (Jonas et al., 2014).

In summary, there are clear lateralising and asymmetrical differences between the left and right visual pathways for higher cortical visual functions but less evidence of laterality for basic retinotopic mapping. Clearly disease can lead to asymmetry, but this remains a relatively unexplored area of research.

# 5. Implications for studies and statistics

*5.1. assumptions of symmetry*

No biological system is likely to produce identical right and left versions, whatever the structure is, but the important question is not 'are they the same' but 'when are they importantly different?'. 'Importantly different' would include, for example, when looking for some association between some feature and the retina, are the results different depending on whether the left or the right eye measures are used in the analysis? We have shown clearly that symmetry of any retinal or ocular structure, or the brain and major vessels to which it is connected, cannot be assumed. Hence until the above question has been answered rigorously, there are many circumstances where use of one eye as a proxy for both eyes is likely to lead to misleading results in a non-systematic and unforeseen manner.

*5.2. "2n eyes of n subjects…"*

The independence of discrete data values within an analysis is essential, if statistical tests are to reasonably represent the sample, and avoid misleading the reader. Non-independence, such as multiple observations from the same individual, create bias within the data, as well as artificially inflating the sample size, which can result in spurious statistical significance (Altman and Bland, 1997). This important concept of 'units of analysis' is particularly relevant to studies involving our eyes, and necessitates caution and consideration before planning ophthalmic studies, as well as in the critical interpretation of published work.

The Ophthalmic Statistics Group is a network of medical statisticians in the UK, engaged in developing standards and improving quality of ophthalmic research. They recognised the importance of the 'units of analysis' issue and addressed it in the first of their published 'Ophthalmic Statistics Notes' (Bunce et al., 2014). Their focus is on studies that involve treatments for ocular disease, and outcome measures, however their advice on avoiding bias and error has wider relevance.

Studies that wish to utilise the data from both eyes of participants need to address the statistical challenges that this produces. Two eyes from one participant cannot be independent subjects, due to the paired cluster bias associated with our eyes being highly similar, and therefore statistical strategies are required to account for this. The choice of how we use both eye data will depend

upon the nature of the study, and whether the observations are subject to confounding from the paired eye.

The Beaver Dam Eye Study used all eyes in their analysis, confirming that "Analyses were done in each eye separately, and relationships between each covariate and retinal thickness measure were modelled using generalized estimating equations with an exchangeable working correlation structure to account for correlation between the 2 eyes from a single participant" (Myers et al., 2015).

Using one eye data per patient avoids this potential for bias, however has the disadvantage of wasting half of the measured data. A UK Biobank study examining associations with macular thickness used one random eye from 32,062 subjects in their analysis (P. J. Patel et al., 2016). Bunce and colleagues suggest we use one random eye from each participant for initial analysis, and the paired eye data as a repeat analysis for validity (Bunce et al., 2014). However, this process assumes a high level of symmetry between the eyes, and we would suggest some modification is needed to this advice.

Armstrong noted the potential for systematic differences between the eyes in his earlier review of ophthalmic studies' handling of eye data (Armstrong, 2013). With increasing evidence of this asymmetry, it is now more important than ever to choose carefully the statistical analysis that is appropriate for the study, considering the emerging evidence for asymmetry between the eyes, in both health and disease.

## 6. Discussion

From the chiral asymmetry of elementary particles to the handedness of biological life of all types from bacteria to humans, where there is apparent symmetry in nature, we can often find asymmetry. In nature we see evidence of adaptation to the environment that necessitates asymmetric physical form, and functional changes (Berg, 1991; Hegstrom and Kondepudi, 1990).

We have known for many centuries the asymmetric location of organs within our bodies. It is not therefore surprising that we can now identify similar systematic (non-random) asymmetry between paired structures at a microscopic level. Our visual system conceals this well within a sensory system that so clearly demonstrates bilaterality, and functions best when right and left are conjugate and integrated.

However, in this review, we have explored how asymmetric our visual system is, with structural and functional differences between left and right sides, both in healthy development and in pathological disease. But more importantly, we have seen how this may be an important developmental adaptation, with greater understanding of the genetic control of patterning during development.

An early understanding of the genetic control of tissue specification and asymmetry in neuronal connectivity came from work with the *Drosophilia* fly (Cutforth and Gaul, 1997; Hsiung and Moses, 2002). Recent work discussed in Section 2 now provides further evidence for asymmetric healthy eye development. Modern genetic and epigenetic theories of biological asymmetry point to left-right patterning and separation at an early embryonic stage, and a prediction that more unilateral genetic diseases will be identified in the future (Ma, 2013).

A plausible explanation (or perhaps consequence) of neuroretinal asymmetry would be sighting ocular dominance, a concept that remains contentious (Mapp et al., 2003), and poorly understood, in the absence of amblyopia, anisometropia or media opacity (Schwartz and Yatziv, 2015). However, ocular dominance is not associated with interocular macula thickness asymmetry (Pekel et al., 2014), but possibly associated with macular GC-IPL thickness (Choi et al., 2016) and RNFL thickness (Choi et al., 2014), although the preponderance for right-sided dominance (in common with motor dominance) is a confounding issue. In fact, work from animal models suggests ocular dominance is a property of the visual cortex, rather than the anterior visual pathway, with recent MRI techniques suggesting this may be true for humans also (Jensen et al.,

2015). Objective measurement or quantification of ocular dominance has proved challenging (Chaumillon et al., 2015) with even visual-evoked potentials (VEPs) proving insufficiently sensitive to assess eye dominance.

We have shown that the order of magnitude of the choice of measurement will influence the precision with which we can identify and measure asymmetry. The evolution of technologies such as OCT is bringing ever greater resolution, and potential to measure microscopic changes within the retina. An inevitable threshold of discrimination will be reached where differences can be detected in all structures, but clearly these differences may be of insignificant magnitude.

Nevertheless, perhaps we should be attempting to quantify the degree of asymmetry in each of the retinal parameters discussed, as a baseline level of asymmetry from which pathology may change this value. Terms such as 'asymmetry index' have an established role in studies of fingerprint asymmetry (Buchwald and Grubska, 2012) and facial attractiveness (Hume and Montgomerie, 2001), where quantitative indices of asymmetry are used to explore relationships with other biological factors, as well as an outcome measure in randomised trials.

Ultimately, we cannot continue to assume symmetry within our eyes and visual pathways. Such assumptions are not only now invalid, but have perhaps been obscuring important findings in eye and brain research.

We need to revisit the development and use of normative data of retinal measures, that are used within OCT devices and similar. Larger sample sizes as well as recognition of interocular asymmetry will provide more meaningful and scientifically valid reference datasets. Equally, the assumption of symmetry cannot be used as a marker of validation or success of new technologies for quantitative imaging of the retina, such as retinal vasculature morphology.

As imaging modalities become more sophisticated in generating long-term data derived from an ever-expanding repertoire of non-invasive tools, it is timely to consider the relevance of both single and paired eye datasets in clinical academic enquiry. In dissecting the determinants of interocular symmetry and neurovascular patterning in development and disease it is clear that there are unanswered questions in how laterality differences might be utilised in research and clinical practice. Researchers should avoid the potential pitfall of forcing an expectation of symmetry on paired structures and clinicians should be aware of both the benefits and limitations in extrapolating single eye data to the fellow eye in diagnosis and prognosis.

## 7. Future Directions

At the heart of understanding biological symmetry is the complex genetic initiation of patterning in development. Biological pruning is a necessary process in neural and vascular morphogenesis in early development and continues throughout life (Watson et al., 2016).

Exploration of the bilateral patterning in post-natal remodelling of the neurovasculature of the retina and visual pathway is required to inform interpretation of variance in symmetry indices which occurs in healthy ageing. The impact of asymmetric retrograde and antegrade influences on both structure and function requires systematic study of the clinical and neuropathologic correlates arising in unhealthy aging and disease. Short and long-term changes occurring over the life course in determining asymmetry in the eye and visual pathway might well be reflective of, and act as a surrogate for understanding brain change. In order to test this hypothesis, the starting point should be to address the question of what signalling pathways and cellular mechanisms drive symmetry and deviations from mirror image mapping in neurovascular morphometry.

This appreciation for the biological processes involved in shaping structural symmetry can underpin the development of ophthalmic imaging devices, that are now so ubiquitous within clinical practice as well research environments. Greater use of captured data will facilitate improved normative datasets, which will in turn provide greater clinical reference.

Finally, from a computational point of view, we see deep learning techniques increasingly making their way into large collections of clinical data (Al-Bander et al., 2016; Fauw et al., 2016; Maninis et al., 2016; Worrall et al., 2016). Our discussion has concentrated on morphology, and ignored a wealth of other and arguably not always independent factors, e.g. haemodynamic and physiological parameters. We have today the tools to take an increasingly holistic view of symmetry, as well as of biomarkers, including a large variety of feature types in the pool of independent variables. Strategies are under way to extract the maximum information from a single patient-imaging episode, providing multi-modal imaging data, and guiding us towards the potential for compound metrics (Cameron et al., 2016). And with large-scale datasets and images now being imported into artificial intelligence systems (Armstrong, 2016), this is only going to grow.

## References


Ahuja, Y., Traboulsi, E.I., 2010. Unilateral megalopapilla and contralateral optic nerve hypoplasia: a case report and review of the literature. J. AAPOS 14, 83–84. doi:10.1016/j.jaapos.2009.10.007

Al-Bander, B., Al-Nuaimy, W., Al-Taee, M., Williams, B., Zheng, Y., 2016. Diabetic Macular Edema Grading Based on Deep Neural Networks, in: Chen, X., Garvin, M., Liu, J., Trucco, E., Xu, Y. (Eds.), Proceedings of the Ophthalmic Medical Image Analysis International Workshop. Athens, pp. 121–128.

Al-Haddad, C., Antonios, R., Tamim, H., Noureddin, B., 2014. Interocular symmetry in retinal and optic nerve parameters in children as measured by spectral domain optical coherence tomography. Br. J. Ophthalmol. 98, 502–506. doi:10.1136/bjophthalmol-2013-304345

Altemir, I., Oros, D., Elía, N., Polo, V., Larrosa, J.M., Pueyo, V., 2013. Retinal asymmetry in children measured with optical coherence tomography. Am. J. Ophthalmol. 156, 1238–1243. doi:10.1016/j.ajo.2013.07.021

Altman, D.G., Bland, J.M., 1997. Statistics Notes: Units of analysis. BMJ 314, 1874. doi:10.1136/bmj.314.7098.1874

Armaly, M.F., 1969. Cup-disc ratio in early open-angle glaucoma. Doc. Ophthalmol. 26, 526–533.

Armstrong, R.A., 2013. Statistical guidelines for the analysis of data obtained from one or both eyes. Ophthalmic Physiol. Opt. 33, 7–14. doi:10.1111/opo.12009

Armstrong, S., 2016. The computer will assess you now. BMJ 355, i5680. doi:10.1136/bmj.i5680

Asefzadeh, B., Cavallerano, A.A., Fisch, B.M., 2007. Racial differences in macular thickness in healthy eyes. Optom. Vis. Sci. 84, 941–945. doi:10.1097/OPX.0b013e318157a6a0

Asil, T., Uzuner, N., 2005. Differentiation of vascular dementia and Alzheimer disease: a functional transcranial Doppler ultrasonographic study. J. Ultrasound Med. 24, 1065–1070.

Asman, P., Heijl, A., 1992. Evaluation of methods for automated Hemifield analysis in perimetry. Arch. Ophthalmol. 110, 820–826. doi:10.1001/archopht.1992.01080180092034

Asrani, S., Rosdahl, J.A., Allingham, R.R., 2011. Novel software strategy for glaucoma

diagnosis: asymmetry analysis of retinal thickness. Arch. Ophthalmol. 129, 1205–1211. doi:10.1001/archophthalmol.2011.242

Avery, R.A., Cnaan, A., Schuman, J.S., Trimboli-Heidler, C., Chen, C.L., Packer, R.J., Ishikawa, H., 2015. Longitudinal Change of Circumpapillary Retinal Nerve Fiber Layer Thickness in Children With Optic Pathway Gliomas. Am J Ophthalmol 160, 944–952. doi:10.1016/j.ajo.2015.07.036

Bachiller, D., Klingensmith, J., Kemp, C., Belo, J.A., Anderson, R.M., May, S.R., McMahon, J.A., McMahon, A.P., Harland, R.M., Rossant, J., De Robertis, E.M., 2000. The organizer factors Chordin and Noggin are required for mouse forebrain development. Nature 403, 658–661. doi:10.1038/35001072

Baker, M.L., Hand, P.J., Wang, J.J., Wong, T.Y., 2008. Retinal signs and stroke: revisiting the link between the eye and brain. Stroke. 39, 1371–1379. doi:10.1161/STROKEAHA.107.496091

Balcer, L.J., Miller, D.H., Reingold, S.C., Cohen, J.A., 2015. Vision and vision-related outcome measures in multiple sclerosis. Brain 138, 11–27. doi:10.1093/brain/awu335

Ballantyne, S.A., O'Neill, G., Hamilton, R., Hollman, A.S., 2002. Observer variation in the sonographic measurement of optic nerve sheath diameter in normal adults. Eur. J. Ultrasound 15, 145–149. doi:10.1016/S0929-8266(02)00036-8

Barondes, M., Pauleikhoff, D., Chisholm, I.C., Minassian, D., Bird, A.C., 1990. Bilaterality of drusen. Br. J. Ophthalmol. 74, 180–182. doi:10.1136/bjo.74.3.180

Bekerman, I., Sigal, T., Kimiagar, I., Ben Ely, A., Vaiman, M., 2016. The quantitative evaluation of intracranial pressure by optic nerve sheath diameter/eye diameter computed tomographic measurement. Am. J. Emerg. Med. S0735-6757. doi:10.1016/j.ajem.2016.08.045

Belecky-Adams, T., Tomarev, S., Li, H.S., Ploder, L., McInnes, R.R., Sundin, O., Adler, R., 1997. Pax-6, Prox 1, and Chx10 homeobox gene expression correlates with phenotypic fate of retinal precursor cells. Invest. Ophthalmol. Vis. Sci. 38, 1293–1303.

Bellmann, C., Jorzik, J., Spital, G., Unnebrink, K., Pauleikhoff, D., Holz, F.G., 2002. Symmetry of bilateral lesions in geographic atrophy in patients with age-related macular degeneration. Arch. Ophthalmol. 120, 579–584. doi:10.1001/archopht.120.5.579

Berg, H.C., 1991. Bacterial motility: handedness and symmetry, in: Bock, G., Marsh, J. (Eds.),

Biological Asymmetry and Handedness. John Wiley & Sons, New York, pp. 58–72.

Bertamini, M., Makin, A., 2014. Brain activity in response to visual symmetry. Symmetry (Basel). 6, 975–996. doi:10.3390/sym6040975

Bland, J.M., Altman, D.G., 1986. Statistical methods for assessing agreement between two methods of clinical measurement. Lancet 1, 307–310. doi:10.1016/S0140-6736(86)90837-8

Böse, J., Gruber, A.D., Helming, L., Schiebe, S., Wegener, I., Hafner, M., Beales, M., Köntgen, F., Lengeling, A., 2004. The phosphatidylserine receptor has essential functions during embryogenesis but not in apoptotic cell removal. J. Biol. 3, 15. doi:10.1186/jbiol10

Bovolenta, P., Mallamaci, A., Puelles, L., Boncinelli, E., 1998. Expression pattern of cSix3, a member of the Six/sine oculis family of transcription factors. Mech. Dev. 70, 201–203. doi:10.1016/S0925-4773(97)00183-4

Brodsky, M.C., 1994. Congenital optic disk anomalies. Surv. Ophthalmol. 39, 89–112. doi:10.1016/0039-6257(94)90155-4

Buchwald, W., Grubska, B., 2012. A complex evaluation of the asymmetry of dermatoglyphs. HOMO - J. Comp. Hum. Biol. 63, 385–395. doi:10.1016/j.jchb.2012.07.002

Budenz, D.L., 2008. Symmetry between the right and left eyes of the normal retinal nerve fiber layer measured with optical coherence tomography (an AOS thesis). Trans. Am. Ophthalmol. Soc. 106, 252–275.

Bunce, C., Patel, K. V, Xing, W., Freemantle, N., Doré, C.J., 2014. Ophthalmic statistics note 1: unit of analysis. Br. J. Ophthalmol. 98, 408–412. doi:10.1136/bjophthalmol-2013-304587

Burmeister, M., Novak, J., Liang, M.Y., Basu, S., Ploder, L., Hawes, N.L., Vidgen, D., Hoover, F., Goldman, D., Kalnins, V.I., Roderick, T.H., Taylor, B.A., Hankin, M.H., McInnes, R.R., 1996. Ocular retardation mouse caused by Chx10 homeobox null allele: impaired retinal progenitor proliferation and bipolar cell differentiation. Nat. Genet. 12, 376–384. doi:10.1038/ng0496-376

Cameron, J.R., Ballerini, L., Langan, C., Warren, C., Denholm, N., Smart, K., MacGillivray, T.J., 2016. Modulation of retinal image vasculature analysis to extend utility and provide secondary value from optical coherence tomography imaging. J Med Imaging 3, 20501. doi:10.1117/1.JMI.3.2.020501

Cameron, J.R., Tatham, A.J., 2016. A window to beyond the orbit: the value of optical coherence

tomography in non-ocular disease. Acta Ophthalmol. 94, 533–539. doi:10.1111/aos.12978

Caramoy, A., Droege, K.M., Kirchhof, B., Fauser, S., 2014. Retinal layers measurements in healthy eyes and in eyes receiving silicone oil-based endotamponade. Acta Ophthalmol. 92, e292-297. doi:10.1111/aos.12307

Cartwright, M.J., Anderson, D.R., 1988. Correlation of asymmetric damage with asymmetric intraocular pressure in normal-tension glaucoma (low-tension glaucoma). Arch. Ophthalmol. 106, 898–900. doi:10.1001/archopht.1988.01060140044020

Chambers, S.M., Fasano, C.A., Papapetrou, E.P., Tomishima, M., Sadelain, M., Studer, L., 2009. Highly efficient neural conversion of human ES and iPS cells by dual inhibition of SMAD signaling. Nat. Biotechnol. 27, 275–280. doi:10.1038/nbt.1529

Chang, B., Yannuzzi, L.A., Ladas, I.D., Guyer, D.R., Slakter, J.S., Sorenson, J.A., 1995. Choroidal neovascularization in second eyes of patients with unilateral exudative age-related macular degeneration. Ophthalmology 102, 1380–1386. doi:10.1016/S0161-6420(95)30860-3

Chang, D.S., Xu, L., Boland, M. V, Friedman, D.S., 2013. Accuracy of pupil assessment for the detection of glaucoma: a systematic review and meta-analysis. Ophthalmology 120, 2217–2225. doi:10.1016/j.ophtha.2013.04.012

Chao, R., Nevin, L., Agarwal, P., Riemer, J., Bai, X., Delaney, A., Akana, M., JimenezLopez, N., Bardakjian, T., Schneider, A., Chassaing, N., Schorderet, D.F., FitzPatrick, D., Kwok, P., Ellgaard, L., Gould, D.B., Zhang, Y., Malicki, J., Baier, H., Slavotinek, A., 2010. A male with unilateral microphthalmia reveals a role for TMX3 in eye development. PLoS One 5, e10565. doi:10.1371/journal.pone.0010565

Chaumillon, R., Alahyane, N., Senot, P., Vergne, J., Lemoine, C., Doré-Mazars, K., Blouin, J., Vergilino-Perez, D., Guillaume, A., 2015. Vers une quantification de la dominance oculaire pour une meilleure prise en charge des pathologies de l'œil. J. Fr. Ophtalmol. 38, 322–332. doi:10.1016/j.jfo.2014.10.009

Cherbuin, N., Réglade-Meslin, C., Kumar, R., Sachdev, P., Anstey, K.J., 2010. Mild Cognitive Disorders are Associated with Different Patterns of Brain asymmetry than Normal Aging: The PATH through Life Study. Front. Psychiatry 1, 11. doi:10.3389/fpsyt.2010.00011

Cheung, N., Mitchell, P., Wong, T.Y., 2010. Diabetic retinopathy. Lancet 376, 124–136.

doi:10.1016/S0140-6736(09)62124-3

Choi, J.A., Kim, J.-S., Jeong, H.J., Lee, J.A., Park, C.K., 2016. Ocular Dominance Is Associated with the Ganglion Cell-Inner Plexiform Layer Thickness Profile in the Macula. PLoS One 11, e0150035. doi:10.1371/journal.pone.0150035

Choi, J.A., Kim, J.-S., Park, H.-Y.L., Park, H., Park, C.K., 2014. Retinal nerve fiber layer thickness profiles associated with ocular laterality and dominance. Neurosci. Lett. 558, 197–202. doi:10.1016/j.neulet.2013.10.054

Chow, R.L., Altmann, C.R., Lang, R.A., Hemmati-Brivanlou, A., 1999. Pax6 induces ectopic eyes in a vertebrate. Development 126, 4213–4222.

Chu, Y., Hughes, S., Chan-Ling, T., 2001. Differentiation and migration of astrocyte precursor cells and astrocytes in human fetal retina: relevance to optic nerve coloboma. FASEB J. 15, 2013–2015. doi:10.1096/fj.00-0868fje

Chuang, J.C., Raymond, P.A., 2001. Zebrafish genes rx1 and rx2 help define the region of forebrain that gives rise to retina. Dev. Biol. 231, 13–30. doi:10.1006/dbio.2000.0125

Cidis, M.B., Warshowsky, J.H., Goldrich, S.G., Meltzer, C.C., 1997. Mirror-image optic nerve dysplasia with associated anisometropia in identical twins. J. Am. Optom. Assoc. 68, 325–329.

Cotton, P.L., Smith, A.T., 2007. Contralateral Visual Hemifield Representations in the Human Pulvinar Nucleus. J. Neurophysiol. 98, 1600–1609. doi:10.1152/jn.00419.2007

Couper, D.J., Klein, R., Hubbard, L.D., Wong, T.Y., Sorlie, P.D., Cooper, L.S., Brothers, R.J., Nieto, F.J., 2002. Reliability of retinal photography in the assessment of retinal microvascular characteristics: the Atherosclerosis Risk in Communities Study. Am. J. Ophthalmol. 133, 78–88. doi:10.1016/S0002-9394(01)01315-0

Curcio, C.A., Allen, K.A., 1990. Topography of ganglion cells in human retina. J. Comp. Neurol. 300, 5–25. doi:10.1002/cne.903000103

Cutforth, T., Gaul, U., 1997. The genetics of visual system development in Drosophila: Specification, connectivity and asymmetry. Curr. Opin. Neurobiol. 7, 48–54. doi:10.1016/S0959-4388(97)80119-5

Dalgliesh, J.D., Tariq, Y.M., Burlutsky, G., Mitchell, P., 2015. Symmetry of retinal parameters measured by spectral-domain OCT in normal young adults. J. Glaucoma 24, 20–24.

doi:10.1097/IJG.0b013e318287ac2f

Danilova, M. V, Mollon, J.D., 2009. The symmetry of visual fields in chromatic discrimination. Brain Cogn. 69, 39–46. doi:10.1016/j.bandc.2008.05.003

Dashtbozorg, B., Mendonça, A.M., Campilho, A., 2014. An automatic graph-based approach for artery/vein classification in retinal images. IEEE Trans. Image Process. 23, 1073–1083. doi:10.1109/TIP.2013.2263809

De Rojas, J.O., Rasool, N., Chen, R.W.S., Horowitz, J., Odel, J.G., 2016. Optical coherence tomography angiography in Leber hereditary optic neuropathy. Neurology 87, 2065–2066. doi:10.1212/WNL.0000000000003313

Dereci, S., Koca, T., Akcam, M., Turkyilmaz, K., 2015. An Evaluation of Peripapillary Retinal Nerve Fiber Layer Thickness in Children With Epilepsy Receiving Treatment of Valproic Acid. Pediatr Neurol 53, 53–57. doi:10.1016/j.pediatrneurol.2015.02.016

Derflinger, S., Sorg, C., Gaser, C., Myers, N., Arsic, M., Kurz, A., Zimmer, C., Wohlschläger, A., Mühlau, M., 2011. Grey-matter atrophy in Alzheimer's disease is asymmetric but not lateralized. J. Alzheimers. Dis. 25, 347–357. doi:10.3233/JAD-2011-110041

Dickie, D.A., Job, D.E., Gonzalez, D.R., Shenkin, S.D., Wardlaw, J.M., 2015. Use of brain MRI atlases to determine boundaries of age-related pathology: the importance of statistical method. PLoS One 10, e0127939. doi:10.1371/journal.pone.0127939

Doubal, F.N., MacGillivray, T.J., Hokke, P.E., Dhillon, B., Dennis, M.S., Wardlaw, J.M., 2009. Differences in retinal vessels support a distinct vasculopathy causing lacunar stroke. Neurology 72, 1773–1778. doi:10.1212/WNL.0b013e3181a60a71

Doubal, F.N., MacGillivray, T.J., Patton, N., Dhillon, B., Dennis, M.S., Wardlaw, J.M., 2010. Fractal analysis of retinal vessels suggests that a distinct vasculopathy causes lacunar stroke. Neurology 74, 1102–1107. doi:10.1212/WNL.0b013e3181d7d8b4

Dreisler, K.K., 1948. Unilateral retinitis pigmentosa; two cases. Acta Ophthalmol. 26, 385–393. doi:10.1111/j.1755-3768.1948.tb07596.x

Dubourg, J., Javouhey, E., Geeraerts, T., Messerer, M., Kassai, B., 2011. Ultrasonography of optic nerve sheath diameter for detection of raised intracranial pressure: a systematic review and meta-analysis. Intensive Care Med. 37, 1059–1068. doi:10.1007/s00134-011-2224-2

Dutton, G.N., 2004. Congenital disorders of the optic nerve: excavations and hypoplasia. Eye 18,

1038–1048. doi:10.1038/sj.eye.6701545

Eidelberg, D., Galaburda, A.M., 1982. Symmetry and asymmetry in the human posterior thalamus. I. Cytoarchitectonic analysis in normal persons. Arch. Neurol. 39, 325–332. doi:10.1001/archneur.1982.00510180003001

El-Ashry, M., Hegde, V., James, P., Pagliarini, S., 2008. Analysis of Macular Thickness in British Population Using Optical Coherence Tomography (OCT): An Emphasis on Interocular Symmetry. Curr. Eye Res. 33, 693–699. doi:10.1080/02713680802323140

Ermakov, A., Stevens, J.L., Whitehill, E., Robson, J.E., Pieles, G., Brooker, D., Goggolidou, P., Powles-Glover, N., Hacker, T., Young, S.R., Dear, N., Hirst, E., Tymowska-Lalanne, Z., Briscoe, J., Bhattacharya, S., Norris, D.P., 2009. Mouse mutagenesis identifies novel roles for left-right patterning genes in pulmonary, craniofacial, ocular, and limb development. Dev. Dyn. 238, 581–594. doi:10.1002/dvdy.21874

Fantes, J., Ragge, N.K., Lynch, S.-A., McGill, N.I., Collin, J.R.O., Howard-Peebles, P.N., Hayward, C., Vivian, A.J., Williamson, K., van Heyningen, V., FitzPatrick, D.R., 2003. Mutations in SOX2 cause anophthalmia. Nat. Genet. 33, 461–463. doi:10.1038/ng1120

Farrell, D.F., 2009. Unilateral retinitis pigmentosa and cone-rod dystrophy. Clin. Ophthalmol. 3, 263–270. doi:10.2147/OPTH.S5130

Fauw, J. De, Keane, P., Tomasev, N., Visentin, D., van den Driessche, G., Johnson, M., Hughes, C., Chu, C., Ledsam, J., Back, T., Peto, T., 2016. Automated analysis of retinal imaging using machine learning techniques for computer vision. F1000Research 5, 1573. doi:10.12688/f1000research.8996.1

Ferda Percin, E., Ploder, L.A., Yu, J.J., Arici, K., Horsford, D.J., Rutherford, A., Bapat, B., Cox, D.W., Duncan, A.M., Kalnins, V.I., Kocak-Altintas, A., Sowden, J.C., Traboulsi, E., Sarfarazi, M., McInnes, R.R., 2000. Human microphthalmia associated with mutations in the retinal homeobox gene CHX10. Nat. Genet. 25, 397–401. doi:10.1038/78071

Field, M.G., Alasil, T., Baniasadi, N., Que, C., Simavli, H., Sobeih, D., Sola-Del Valle, D., Best, M.J., Chen, T.C., 2016. Facilitating Glaucoma Diagnosis With Intereye Retinal Nerve Fiber Layer Asymmetry Using Spectral-Domain Optical Coherence Tomography. J. Glaucoma 25, 167–176. doi:10.1097/IJG.0000000000000080

Fleckenstein, M., Maumenee, I.H., 2005. Unilateral isolated microphthalmia inherited as an

autosomal recessive trait. Ophthalmic Genet. 26, 163–168. doi:10.1080/13816810500468672

Foerch, C., Misselwitz, B., Sitzer, M., Berger, K., Steinmetz, H., Neumann-Haefelin, T., 2005. Difference in recognition of right and left hemispheric stroke. Lancet 366, 392–393. doi:10.1016/S0140-6736(05)67024-9

Forooghian, F., Cukras, C., Meyerle, C.B., Chew, E.Y., Wong, W.T., 2008. Evaluation of time domain and spectral domain optical coherence tomography in the measurement of diabetic macular edema. Invest. Ophthalmol. Vis. Sci. 49, 4290–4296. doi:10.1167/iovs.08-2113

Franceschetti, A., Bock, R., 1950. Megalopapilla; a new congenital anomaly. Am. J. Ophthalmol. 33, 227–235.

Francois, J., Verriest, G., 1952. Retinopathie pigmentaire unilaterale. Ophthalmologica 124, 65–87. doi:10.1159/000301252

Frasnelli, E., 2013. Brain and behavioral lateralization in invertebrates. Front. Psychol. 4, 939. doi:10.3389/fpsyg.2013.00939

Furukawa, T., Morrow, E.M., Cepko, C.L., 1997. Crx, a novel otx-like homeobox gene, shows photoreceptor-specific expression and regulates photoreceptor differentiation. Cell 91, 531–541. doi:10.1016/S0092-8674(00)80439-0

Gangnon, R.E., Lee, K.E., Klein, B.E.K., Iyengar, S.K., Sivakumaran, T.A., Klein, R., 2015. Severity of age-related macular degeneration in 1 eye and the incidence and progression of age-related macular degeneration in the fellow eye: the Beaver Dam Eye Study. JAMA Ophthalmol. 133, 125–132. doi:10.1001/jamaophthalmol.2014.4252

Gass, J.D., 1972. Drusen and disciform macular detachment and degeneration. Trans. Am. Ophthalmol. Soc. 70, 409–436. doi:10.1001/archopht.1973.01000050208006

Gauvin, M., Chakor, H., Koenekoop, R.K., Little, J.M., Lina, J.-M., Lachapelle, P., 2016. Witnessing the first sign of retinitis pigmentosa onset in the allegedly normal eye of a case of unilateral RP: a 30-year follow-up. Doc. Ophthalmol. 132, 213–229. doi:10.1007/s10633-016-9537-y

Gemenetzi, M., Lotery, A.J., 2014. The role of epigenetics in age-related macular degeneration. Eye 28, 1407–1417. doi:10.1038/eye.2014.225

Giger-Tobler, C., Eisenack, J., Holzmann, D., Pangalu, A., Sturm, V., Killer, H.E., Landau, K.,

Jaggi, G.P., 2015. Measurement of Optic Nerve Sheath Diameter: Differences between Methods? A Pilot Study. Klin. Monbl. Augenheilkd. 232, 467–470. doi:10.1055/s-0035-1545711

Giurfa, M., Zhang, S., Jenett, A., Menzel, R., Srinivasan, M. V, 2001. The concepts of "sameness" and "difference" in an insect. Nature 410, 930–933. doi:10.1038/35073582

Golnik, K.C., Hund, P.W., Stroman, G.A., Stewart, W.C., 1996. Magnetic resonance imaging in patients with unexplained optic neuropathy. Ophthalmology 103, 515–520. doi:10.1016/S0161-6420(96)30664-7

Gracitelli, C.P.B., Tatham, A.J., Zangwill, L.M., Weinreb, R.N., Abe, R.Y., Diniz-Filho, A., Paranhos, A., Baig, S., Medeiros, F.A., 2016. Asymmetric Macular Structural Damage Is Associated With Relative Afferent Pupillary Defects in Patients With Glaucoma. Invest. Ophthalmol. Vis. Sci. 57, 1738–1746. doi:10.1167/iovs.15-18079

Greenfield, D.S., Liebmann, J.M., Ritch, R., Krupin, T., Low-Pressure Glaucoma Study Group, 2007. Visual field and intraocular pressure asymmetry in the low-pressure glaucoma treatment study. Ophthalmology 114, 460–465. doi:10.1016/j.ophtha.2006.06.056

Grindley, J.C., Davidson, D.R., Hill, R.E., 1995. The role of Pax-6 in eye and nasal development. Development 121, 1433–1442.

Grover, S., Murthy, R.K., Brar, V.S., Chalam, K. V., 2009. Normative Data for Macular Thickness by High-Definition Spectral-Domain Optical Coherence Tomography (Spectralis). Am. J. Ophthalmol. 148, 266–271. doi:10.1016/j.ajo.2009.03.006

Gugleta, K., Orgül, S., Flammer, J., 1999. Asymmetry in intraocular pressure and retinal nerve fiber layer thickness in normal-tension glaucoma. Ophthalmologica. 213, 219–223. doi:10.1159/000027425

Ha, D.-W., Sung, K., Kim, S., Park, R., Kim, K., Kook, M.S., 2002. Interocular comparison of nerve fiber layer thickness and its relation with optic disc size in normal subjects. Korean J. Ophthalmol. 16, 8–12. doi:10.3341/kjo.2002.16.1.8

Hao, H., Sasongko, M.B., Wong, T.Y., Che Azemin, M.Z., Aliahmad, B., Hodgson, L., Kawasaki, R., Cheung, C.Y., Wang, J.J., Kumar, D.K., 2012. Does retinal vascular geometry vary with cardiac cycle? Investig. Ophthalmol. Vis. Sci. 53, 5799–5805. doi:10.1167/iovs.11-9326

Hart, N.S., Partridge, J.C., Cuthill, I.C., 2000. Retinal asymmetry in birds. Curr. Biol. 10, 115–117. doi:10.1016/S0960-9822(00)00297-9

Hatta, K., Kimmel, C.B., Ho, R.K., Walker, C., 1991. The cyclops mutation blocks specification of the floor plate of the zebrafish central nervous system. Nature 350, 339–341. doi:10.1038/350339a0

Hedna, V.S., Bodhit, A.N., Ansari, S., Falchook, A.D., Stead, L., Heilman, K.M., Waters, M.F., 2013. Hemispheric Differences in Ischemic Stroke: Is Left-Hemisphere Stroke More Common? J. Clin. Neurol. 9, 97–102. doi:10.3988/jcn.2013.9.2.97

Hegstrom, R., Kondepudi, D., 1990. The handedness of the universe. Sci. Am. 262, 108–115. doi:10.1038/scientificamerican0190-108

Heisenberg, C.P., Houart, C., Take-Uchi, M., Rauch, G.J., Young, N., Coutinho, P., Masai, I., Caneparo, L., Concha, M.L., Geisler, R., Dale, T.C., Wilson, S.W., Stemple, D.L., 2001. A mutation in the Gsk3-binding domain of zebrafish Masterblind/Axin1 leads to a fate transformation of telencephalon and eyes to diencephalon. Genes Dev. 15, 1427–1434. doi:10.1101/gad.194301

Hood, D.C., Raza, A.S., de Moraes, C.G. V, Liebmann, J.M., Ritch, R., 2013. Glaucomatous damage of the macula. Prog. Retin. Eye Res. 32, 1–21. doi:10.1016/j.preteyeres.2012.08.003

Houart, C., Caneparo, L., Heisenberg, C., Barth, K., Take-Uchi, M., Wilson, S., 2002. Establishment of the telencephalon during gastrulation by local antagonism of Wnt signaling. Neuron 35, 255–265. doi:10.1016/S0896-6273(02)00751-1

Hougaard, A., Jensen, B.H., Amin, F.M., Rostrup, E., Hoffmann, M.B., Ashina, M., 2015. Cerebral Asymmetry of fMRI-BOLD Responses to Visual Stimulation. PLoS One 10, e0126477. doi:10.1371/journal.pone.0126477

Hsiung, F., Moses, K., 2002. Retinal development in Drosophila: specifying the first neuron. Hum. Mol. Genet. 11, 1207–1214. doi:10.1093/hmg/11.10.1207

Huang, D., Swanson, E.A., Lin, C.P., Schuman, J.S., Stinson, W.G., Chang, W., Hee, M.R., Flotte, T., Gregory, K., Puliafito, C.A., et al., 1991. Optical coherence tomography. Science (80-. ). 254, 1178–1181.

Hume, D.K., Montgomerie, R., 2001. Facial attractiveness signals different aspects of “quality” in women and men. Evol. Hum. Behav. 22, 93–112. doi:10.1016/S1090-5138(00)00065-9

Huynh, S.C., Wang, X.Y., Burlutsky, G., Mitchell, P., 2007. Symmetry of Optical Coherence Tomography Retinal Measurements in Young Children. Am. J. Ophthalmol. 143, 518–520. doi:10.1016/j.ajo.2006.09.050

Hwang, Y.H., Song, M., Kim, Y.Y., Yeom, D.J., Lee, J.H., 2014. Interocular symmetry of retinal nerve fibre layer thickness in healthy eyes: a spectral-domain optical coherence tomographic study. Clin. Exp. Optom. 97, 550–554. doi:10.1111/cxo.12218

Jacobsen, A.G., Bendtsen, M.D., Vorum, H., Bøgsted, M., Hargitai, J., 2015. Normal Value Ranges for Central Retinal Thickness Asymmetry in Healthy Caucasian Adults Measured by SPECTRALIS SD-OCT Posterior Pole Asymmetry Analysis. Invest. Ophthalmol. Vis. Sci. 56, 3875–3882. doi:10.1167/iovs.14-15663

Jensen, B.H., Hougaard, A., Amin, F.M., Larsson, H.B.W., Ashina, M., 2015. Structural asymmetry of cortical visual areas is related to ocular dominance. Neuroreport 26, 1071–1076. doi:10.1097/WNR.0000000000000470

Jonas, J., Frismand, S., Vignal, J.-P., Colnat-Coulbois, S., Koessler, L., Vespignani, H., Rossion, B., Maillard, L., 2014. Right hemispheric dominance of visual phenomena evoked by intracerebral stimulation of the human visual cortex. Hum. Brain Mapp. 35, 3360–3371. doi:10.1002/hbm.22407

Joseph, R., 1951. Unilateral retinitis pigmentosa. Br. J. Ophthalmol. 35, 98–113.

Kalantari, H., Jaiswal, R., Bruck, I., Matari, H., Ghobadi, F., Weedon, J., Hassen, G.W., 2013. Correlation of optic nerve sheath diameter measurements by computed tomography and magnetic resonance imaging. Am. J. Emerg. Med. 31, 1595–1597. doi:10.1016/j.ajem.2013.07.028

Kaplowitz, K., Blizzard, S., Blizzard, D.J., Nwogu, E., Hamill, C.E., Weinreb, R.N., Mohsenin, V., Loewen, N.A., 2015. Time Spent in Lateral Sleep Position and Asymmetry in Glaucoma. Invest. Ophthalmol. Vis. Sci. 56, 3869–3874. doi:10.1167/iovs.14-16079

Karim, S., Clark, R.A., Poukens, V., Demer, J.L., 2004. Demonstration of systematic variation in human intraorbital optic nerve size by quantitative magnetic resonance imaging and histology. Invest. Ophthalmol. Vis. Sci. 45, 1047–1051. doi:10.1167/iovs.03-1246

Kass, M.A., Heuer, D.K., Higginbotham, E.J., Johnson, C.A., Keltner, J.L., Miller, J.P., Parrish, R.K., Wilson, M.R., Gordon, M.O., 2002. The Ocular Hypertension Treatment Study: a

randomized trial determines that topical ocular hypotensive medication delays or prevents the onset of primary open-angle glaucoma. Arch. Ophthalmol. 120, 701–713. doi:10.1001/archopht.120.6.701

Kastner, S., O'Connor, D.H., Fukui, M.M., Fehd, H.M., Herwig, U., Pinsk, M.A., 2004. Functional imaging of the human lateral geniculate nucleus and pulvinar. J. Neurophysiol. 91, 438–448. doi:10.1152/jn.00553.2003

Kawakami, Y., Raya, A., Raya, R.M., Rodríguez-Esteban, C., Izpisúa Belmonte, J.C., 2005. Retinoic acid signalling links left-right asymmetric patterning and bilaterally symmetric somitogenesis in the zebrafish embryo. Nature 435, 165–171. doi:10.1038/nature03512

Keane, P.A., Grossi, C.M., Foster, P.J., Yang, Q., Reisman, C.A., Chan, K., Peto, T., Thomas, D., Patel, P.J., 2016. Optical Coherence Tomography in the UK Biobank Study – Rapid Automated Analysis of Retinal Thickness for Large Population-Based Studies. PLoS One 11, e0164095. doi:10.1371/journal.pone.0164095

Kelty, P.J., Payne, J.F., Trivedi, R.H., Kelty, J., Bowie, E.M., Burger, B.M., 2008. Macular Thickness Assessment in Healthy Eyes Based on Ethnicity Using Stratus OCT Optical Coherence Tomography. Investig. Opthalmology Vis. Sci. 49, 2668. doi:10.1167/iovs.07-1000

Kennedy, D.N., O'Craven, K.M., Ticho, B.S., Goldstein, A.M., Makris, N., Henson, J.W., 1999. Structural and functional brain asymmetries in human situs inversus totalis. Neurology 53, 1260–1265. doi:10.1212/WNL.53.6.1260

Kertesz, A., Black, S.E., Polk, M., Howell, J., 1986. Cerebral asymmetries on magnetic resonance imaging. Cortex. 22, 117–127. doi:10.1016/S0010-9452(86)80036-3

Kim, T.-W., Hwang, J.-M., 2007. Stratus OCT in Dominant Optic Atrophy. J. Glaucoma 16, 655–658. doi:10.1097/IJG.0b013e31804d23aa

Kirkman, M.A., Yu-Wai-Man, P., Korsten, A., Leonhardt, M., Dimitriadis, K., De Coo, I.F., Klopstock, T., Chinnery, P.F., 2009. Gene-environment interactions in Leber hereditary optic neuropathy. Brain 132, 2317–2326. doi:10.1093/brain/awp158

Klein, R., Sharrett, A.R., Klein, B.E., Chambless, L.E., Cooper, L.S., Hubbard, L.D., Evans, G., 2000. Are retinal arteriolar abnormalities related to atherosclerosis?: The Atherosclerosis Risk in Communities Study. Arterioscler. Thromb. Vasc. Biol. 20, 1644–1650.

doi:10.1161/01.ATV.20.6.1644

Knudtson, M.D., Klein, B.E.K., Klein, R., Wong, T.Y., Hubbard, L.D., Lee, K.E., Meuer, S.M., Bulla, C.P., 2004. Variation associated with measurement of retinal vessel diameters at different points in the pulse cycle. Br. J. Ophthalmol. 88, 57–61. doi:10.1136/bjo.88.1.57

Kolb, H., Galloway, N.R., 1964. Three cases of unilateral pigmentary degeneration. Br. J. Ophthalmol. 48, 471–479.

Kronmal, R.A., 1993. Spurious Correlation and the Fallacy of the Ratio Standard Revisited. J. R. Stat. Soc. 156, 379. doi:10.2307/2983064

Kurimoto, Y., Matsuno, K., Kaneko, Y., Umihira, J., Yoshimura, N., 2000. Asymmetries of the retinal nerve fibre layer thickness in normal eyes. Br. J. Ophthalmol. 84, 469–472. doi:10.1136/bjo.84.5.469

Lavin, M.J., Eldem, B., Gregor, Z.J., 1991. Symmetry of disciform scars in bilateral age-related macular degeneration. Br. J. Ophthalmol. 75, 133–136. doi:10.1136/bjo.75.3.133

Le May, M., Kido, D.K., 1978. Asymmetries of the cerebral hemispheres on computed tomograms. J. Comput. Assist. Tomogr. 2, 471–476.

Lee, A.J., Wang, J.J., Rochtchina, E., Healey, P., Chia, E.-M., Mitchell, P., 2003. Patterns of glaucomatous visual field defects in an older population: the Blue Mountains Eye Study. Clin. Experiment. Ophthalmol. 31, 331–335. doi:10.1046/j.1442-9071.2003.00660.x

Lee, S.Y., Jeoung, J.W., Park, K.H., Kim, D.M., 2015. Macular ganglion cell imaging study: Interocular symmetry of ganglion cell-inner plexiform layer thickness in normal healthy eyes. Am. J. Ophthalmol. 159, 315–323.e2. doi:10.1016/j.ajo.2014.10.032

Letzkus, P., Boeddeker, N., Wood, J.T., Zhang, S.-W., Srinivasan, M. V, 2008. Lateralization of visual learning in the honeybee. Biol. Lett. 4, 16–18. doi:10.1098/rsbl.2007.0466

Leung, A.K.C., Fong, J.H.S., Leong, A.G., 2002. Hemihypertrophy. J. R. Soc. Promot. Health 122, 24–27. doi:10.1177/146642400212200111

Leung, C.K.S., Ye, C., Weinreb, R.N., Yu, M., Lai, G., Lam, D.S., 2013. Impact of age-related change of retinal nerve fiber layer and macular thicknesses on evaluation of glaucoma progression. Ophthalmology 120, 2485–2492. doi:10.1016/j.ophtha.2013.07.021

Leung, C.K.S., Yu, M., Weinreb, R.N., Ye, C., Liu, S., Lai, G., Lam, D.S.C., 2012. Retinal nerve

fiber layer imaging with spectral-domain optical coherence tomography: a prospective analysis of age-related loss. Ophthalmology 119, 731–737. doi:10.1016/j.ophtha.2011.10.010

Leung, H., Wang, J.J., Rochtchina, E., Tan, A.G., Wong, T.Y., Hubbard, L.D., Klein, R., Mitchell, P., 2003. Computer-assisted retinal vessel measurement in an older population: correlation between right and left eyes. Clin. Experiment. Ophthalmol. 31, 326–330. doi:10.1046/j.1442-9071.2003.00661.x

Levin, M., 2005. Left-right asymmetry in embryonic development: a comprehensive review. Mech. Dev. 122, 3–25. doi:10.1016/j.mod.2004.08.006

Levine, R.A., Demirel, S., Fan, J., Keltner, J.L., Johnson, C.A., Kass, M.A., Ocular Hypertension Treatment Study Group, 2006. Asymmetries and visual field summaries as predictors of glaucoma in the ocular hypertension treatment study. Invest. Ophthalmol. Vis. Sci. 47, 3896–3903. doi:10.1167/iovs.05-0469

Lewis, S.C., Wardlaw, J.M., 2002. Which Doppler velocity is best for assessing suitability for carotid endarterectomy? Eur. J. Ultrasound 15, 9–20. doi:10.1016/S0929-8266(01)00168-9

Li, H., Healey, P.R., Tariq, Y.M., Teber, E., Mitchell, P., 2013. Symmetry of optic nerve head parameters measured by the heidelberg retina tomograph 3 in healthy eyes: the Blue Mountains Eye study. Am. J. Ophthalmol. 155, 518–523.e1. doi:10.1016/j.ajo.2012.09.019

Li, H., Tierney, C., Wen, L., Wu, J.Y., Rao, Y., 1997. A single morphogenetic field gives rise to two retina primordia under the influence of the prechordal plate. Development 124, 603–615.

Liew, G., Wang, J.J., 2011. Retinal vascular signs: a window to the heart?. Rev. Esp. Cardiol. 64, 515–521. doi:10.1016/j.recesp.2011.02.014

Liu, I.S., Chen, J.D., Ploder, L., Vidgen, D., van der Kooy, D., Kalnins, V.I., McInnes, R.R., 1994. Developmental expression of a novel murine homeobox gene (Chx10): evidence for roles in determination of the neuroretina and inner nuclear layer. Neuron 13, 377–393. doi:10.1016/0896-6273(94)90354-9

Liu, J.H.K., Weinreb, R.N., 2014. Asymmetry of habitual 24-hour intraocular pressure rhythm in glaucoma patients. Invest. Ophthalmol. Vis. Sci. 55, 7398–7402. doi:10.1167/iovs.14-14464

Liu, T., Hu, A.Y., Kaines, A., Yu, F., Schwartz, S.D., Hubschman, J.-P., 2011. A Pilot Study of

Normative Data for Macular Thickness and Volume Measurements Using Cirrus High-Definition Optical Coherence Tomography. Retina 31, 1944–1950. doi:10.1097/IAE.0b013e31820d3f13

Lombardo, M., Lombardo, G., Schiano Lomoriello, D., Ducoli, P., Stirpe, M., Serrao, S., 2013. Interocular symmetry of parafoveal photoreceptor cone density distribution. Retina 33, 1640–1649. doi:10.1097/IAE.0b013e3182807642

London, A., Benhar, I., Schwartz, M., 2013. The retina as a window to the brain-from eye research to CNS disorders. Nat. Rev. Neurol. 9, 44–53. doi:10.1038/nrneurol.2012.227

Loosli, F., Winkler, S., Wittbrodt, J., 1999. Six3 overexpression initiates the formation of ectopic retina. Genes Dev. 13, 649–654.

Lu, M.F., Pressman, C., Dyer, R., Johnson, R.L., Martin, J.F., 1999. Function of Rieger syndrome gene in left-right asymmetry and craniofacial development. Nature 401, 276–278. doi:10.1038/45797

Ludbrook, J., 2002. Statistical techniques for comparing measurers and methods of measurement: a critical review. Clin. Exp. Pharmacol. Physiol. 29, 527–536. doi:10.1046/j.1440-1681.2002.03686.x

Lupo, G., Bertacchi, M., Carucci, N., Augusti-Tocco, G., Biagioni, S., Cremisi, F., 2014. From pluripotency to forebrain patterning: an in vitro journey astride embryonic stem cells. Cell. Mol. Life Sci. 71, 2917–2930. doi:10.1007/s00018-014-1596-1

Ma, K., 2013. Embryonic left-right separation mechanism allows confinement of mutation-induced phenotypes to one lateral body half of bilaterians. Am. J. Med. Genet. 161A, 3095–3114. doi:10.1002/ajmg.a.36188

Macdonald, R., Barth, K.A., Xu, Q., Holder, N., Mikkola, I., Wilson, S.W., 1995. Midline signalling is required for Pax gene regulation and patterning of the eyes. Development 121, 3267–3278.

MacGillivray, T.J., Cameron, J.R., Zhang, Q., El-Medany, A., Mulholland, C., Sheng, Z., Dhillon, B., Doubal, F.N., Foster, P.J., Trucco, E., Sudlow, C., Consortium, U.K.B.E., Vision, 2015. Suitability of UK Biobank Retinal Images for Automatic Analysis of Morphometric Properties of the Vasculature. PLoS One 10, e0127914. doi:10.1371/journal.pone.0127914

MacGillivray, T.J., Trucco, E., Cameron, J.R., Dhillon, B., Houston, J.G., van Beek, E.J., 2014. Retinal imaging as a source of biomarkers for diagnosis, characterization and prognosis of chronic illness or long-term conditions. Br J Radiol 87, 20130832. doi:10.1259/bjr.20130832

Mahroo, O.A., Mitry, D., Williamson, T.H., Shepherd, A., Charteris, D.G., Hamilton, R.D., 2015. Exploring Sex and Laterality Imbalances in Patients Undergoing Laser Retinopexy. JAMA Ophthalmol. 133, 1334–1336. doi:10.1001/jamaophthalmol.2015.2731

Maisel, J.M., Pearlstein, C.S., Adams, W.H., Heotis, P.M., 1989. Large optic disks in the Marshallese population. Am. J. Ophthalmol. 107, 145–150. doi:10.1016/0002-9394(89)90213-4

Maninis, K., Pont-Tuset, J., Arbeláez, P., 2016. Deep retinal image understanding, in: Ourselin, S., Joskowicz, L., Sabunca, M., Unal, G., Wells, W. (Eds.), International Conference on Medical Image Computing and Computer-Assisted Intervention. Springer International, Athens, pp. 140–148.

Mann, S.S., Rutishauser-Arnold, Y., Peto, T., Jenkins, S.A., Leung, I., Xing, W., Bird, A.C., Bunce, C., Webster, A.R., 2011. The symmetry of phenotype between eyes of patients with early and late bilateral age-related macular degeneration (AMD). Graefes Arch. Clin. Exp. Ophthalmol. 249, 209–214. doi:10.1007/s00417-010-1483-x

Mapp, A., Ono, H., Barbeito, R., 2003. What does the dominant eye dominate? A brief and somewhat contentious review. Percept. Psychophys. 65, 310–317. doi:10.3758/BF03194802

Marsiglia, M., Duncker, T., Peiretti, E., Brodie, S.E., Tsang, S.H., 2012. Unilateral retinitis pigmentosa: a proposal of genetic pathogenic mechanisms. Eur. J. Ophthalmol. 22, 654–660. doi:10.5301/ejo.5000086

Mathers, P.H., Grinberg, A., Mahon, K.A., Jamrich, M., 1997. The Rx homeobox gene is essential for vertebrate eye development. Nature 387, 603–607. doi:10.1038/42475

Medeiros, F.A., Zangwill, L.M., Bowd, C., Vessani, R.M., Susanna, R., Weinreb, R.N., 2005. Evaluation of retinal nerve fiber layer, optic nerve head, and macular thickness measurements for glaucoma detection using optical coherence tomography. Am. J. Ophthalmol. 139, 44–55. doi:10.1016/j.ajo.2004.08.069

Megaw, R.D., Lampe, A., Dhillon, B., Yoshida, S., Wright, A.F., 2013. Papillorenal syndrome in

a family with unusual complications. Br. J. Ophthalmol. 97, 945–946. doi:10.1136/bjophthalmol-2013-303122

Mehra, K.S., 1962. Unilateral retinitis pigmentosa. Br. J. Ophthalmol. 46, 310.

Mitry, D., Tuft, S., McLeod, D., Charteris, D.G., 2011. Laterality and gender imbalances in retinal detachment. Graefe's Arch. Clin. Exp. Ophthalmol. 249, 1109–1110. doi:10.1007/s00417-010-1529-0

Moore, G.H., Bowd, C., Medeiros, F.A., Sample, P.A., Liebmann, J.M., Girkin, C.A., Leite, M.T., Weinreb, R.N., Zangwill, L.M., 2013. African descent and glaucoma evaluation study: asymmetry of structural measures in normal participants. J. Glaucoma 22, 65–72. doi:10.1097/IJG.0b013e31822e8e51

Mukhopadhyay, R., Holder, G.E., Moore, A.T., Webster, A.R., 2011. Unilateral retinitis pigmentosa occurring in an individual with a germline mutation in the RP1 gene. Arch. Ophthalmol. 129, 954–956. doi:10.1001/archophthalmol.2011.171

Murray, G.D., Miller, R., 1990. Statistical comparison of two methods of clinical measurement. Br. J. Surg. 77, 385–387. doi:10.1002/bjs.1800770410

Mwanza, J.-C., Durbin, M.K., Budenz, D.L., Cirrus OCT Normative Database Study Group, 2011. Interocular symmetry in peripapillary retinal nerve fiber layer thickness measured with the Cirrus HD-OCT in healthy eyes. Am. J. Ophthalmol. 151, 514–521.e1. doi:10.1016/j.ajo.2010.09.015

Myers, C.E., Klein, B.E.K., Meuer, S.M., Swift, M.K., Chandler, C.S., Huang, Y., Gangaputra, S., Pak, J.W., Danis, R.P., Klein, R., 2015. Retinal Thickness Measured by Spectral-Domain Optical Coherence Tomography in Eyes Without Retinal Abnormalities: The Beaver Dam Eye Study. Am. J. Ophthalmol. 159, 445–456.e1. doi:10.1016/j.ajo.2014.11.025

Newbury-Ecob, R.A., Leanage, R., Raeburn, J.A., Young, I.D., 1996. Holt-Oram syndrome: a clinical genetic study. J. Med. Genet. 33, 300–307. doi:10.1136/jmg.33.4.300

Newman, W.D., Hollman, A.S., Dutton, G.N., Carachi, R., 2002. Measurement of optic nerve sheath diameter by ultrasound: a means of detecting acute raised intracranial pressure in hydrocephalus. Br. J. Ophthalmol. 86, 1109–1113. doi:10.1136/bjo.86.10.1109

Nikoskelainen, E.K., Huoponen, K., Juvonen, V., Lamminen, T., Nummelin, K., Savontaus, M.L., 1996. Ophthalmologic findings in Leber hereditary optic neuropathy, with special

reference to mtDNA mutations. Ophthalmology 103, 504–514. doi:10.1016/S0161-6420(96)30665-9

Nordstrand, L.M., Svärd, J., Larsen, E., Nilsen, A., Ougland, R., Furu, K., Lien, G.F., Rognes, T., Namekawa, S.H., Lee, J.T., Klungland, A., 2010. Mice lacking Alkbh1 display sex-ratio distortion and unilateral eye defects. PLoS One 5, e13827. doi:10.1371/journal.pone.0013827

Ohden, K.L., Tang, P.H., Lilley, C.C., Lee, M.S., 2016. Atypical Leber Hereditary Optic Neuropathy. J. Neuro-Ophthalmology 36, 304. doi:10.1097/WNO.0000000000000346

Okada, N., Takagi, Y., Seikai, T., Tanaka, M., Tagawa, M., 2001. Asymmetrical development of bones and soft tissues during eye migration of metamorphosing Japanese flounder, Paralichthys olivaceus. Cell Tissue Res. 304, 59–66. doi:10.1007/s004410100353

Okamoto, F., Nonoyama, T., Hommura, S., 2001. Mirror image myopic anisometropia in two pairs of monozygotic twins. Ophthalmologica. 215, 435–438. doi:10.1159/000050904

Ong, L.S., Mitchell, P., Healey, P.R., Cumming, R.G., 1999. Asymmetry in optic disc parameters: the Blue Mountains Eye Study. Invest. Ophthalmol. Vis. Sci. 40, 849–857.

Optic Neuritis Study Group., 1991. The clinical profile of optic neuritis. Experience of the Optic Neuritis Treatment Trial. Arch. Ophthalmol. 109, 1673–1678. doi:10.1001/archopht.1991.01080120057025

Özer, C.M., Öz, I.I., Şerifoğlu, I., Büyükuysal, M.Ç., Barut, Ç., 2016. Evaluation of Eyeball and Orbit in Relation to Gender and Age. J. Craniofac. Surg. 27, e793-800. doi:10.1097/SCS.0000000000003133

Park, J.J., Oh, D.R., Hong, S.P., Lee, K.W., 2005. Asymmetry analysis of the retinal nerve fiber layer thickness in normal eyes using optical coherence tomography. Korean J. Ophthalmol. 19, 281–287. doi:10.3341/kjo.2005.19.4.281

Pasutto, F., Sticht, H., Hammersen, G., Gillessen-Kaesbach, G., Fitzpatrick, D.R., Nürnberg, G., Brasch, F., Schirmer-Zimmermann, H., Tolmie, J.L., Chitayat, D., Houge, G., Fernández-Martínez, L., Keating, S., Mortier, G., Hennekam, R.C.M., von der Wense, A., Slavotinek, A., Meinecke, P., Bitoun, P., Becker, C., Nürnberg, P., Reis, A., Rauch, A., 2007. Mutations in STRA6 cause a broad spectrum of malformations including anophthalmia, congenital heart defects, diaphragmatic hernia, alveolar capillary dysplasia, lung hypoplasia, and

mental retardation. Am. J. Hum. Genet. 80, 550–560. doi:10.1086/512203

Patel, A., Purohit, R., Lee, H., Sheth, V., Maconachie, G., Papageorgiou, E., McLean, R.J., Gottlob, I., Proudlock, F.A., 2016. Optic Nerve Head Development in Healthy Infants and Children Using Handheld Spectral-Domain Optical Coherence Tomography. Ophthalmology 123, 2147–2157. doi:10.1016/j.ophtha.2016.06.057

Patel, P.J., Foster, P.J., Grossi, C.M., Keane, P.A., Ko, F., Lotery, A., Peto, T., Reisman, C.A., Strouthidis, N.G., Yang, Q., UK Biobank Eyes and Vision Consortium, 2016. Spectral-Domain Optical Coherence Tomography Imaging in 67 321 Adults: Associations with Macular Thickness in the UK Biobank Study. Ophthalmology 123, 829–840. doi:10.1016/j.ophtha.2015.11.009

Patton, N., Aslam, T., Macgillivray, T., Pattie, A., Deary, I.J., Dhillon, B., 2005. Retinal vascular image analysis as a potential screening tool for cerebrovascular disease: a rationale based on homology between cerebral and retinal microvasculatures. J Anat 206, 319–348. doi:10.1111/j.1469-7580.2005.00395.x

Patton, Aslam, T., Murray, G., 2006a. Statistical strategies to assess reliability in ophthalmology. Eye 20, 749–754. doi:10.1038/sj.eye.6702097

Patton, Aslam, T.M., MacGillivray, T., Deary, I.J., Dhillon, B., Eikelboom, R.H., Yogesan, K., Constable, I.J., 2006b. Retinal image analysis: Concepts, applications and potential. Prog. Retin. Eye Res. 25, 99–127. doi:10.1016/j.preteyeres.2005.07.001

Paulozzi, L.J., Lary, J.M., 1999. Laterality patterns in infants with external birth defects. Teratology 60, 265–271. doi:10.1002/(SICI)1096-9926(199911)60:5<265::AID-TERA7>3.0.CO;2-H

Pekel, G., Acer, S., Özbakis, F., Yagci, R., Sayin, N., 2014. Macular asymmetry analysis in sighting ocular dominance. Kaohsiung J. Med. Sci. 30, 531–536. doi:10.1016/j.kjms.2014.08.003

Pellegrini, E., Robertson, G., Trucco, E., MacGillivray, T.J., Lupascu, C., van Hemert, J., Williams, M.C., Newby, D.E., van Beek, E., Houston, G., 2014. Blood vessel segmentation and width estimation in ultra-wide field scanning laser ophthalmoscopy. Biomed. Opt. Express 5, 4329–4337. doi:10.1364/BOE.5.004329

Perez-Rovira, A., MacGillivray, T., Trucco, E., Chin, K.S., Zutis, K., Lupascu, C., Tegolo, D.,

Giachetti, A., Wilson, P.J., Doney, A., Dhillon, B., 2011. VAMPIRE: Vessel Assessment and Measurement Platform for Images of the REtina. Conf Proc IEEE Eng Med Biol Soc 2011, 3391–3394. doi:10.1109/iembs.2011.6090918

Portegies, M.L.P., Selwaness, M., Hofman, A., Koudstaal, P.J., Vernooij, M.W., Ikram, M.A., 2015. Left-Sided Strokes Are More Often Recognized Than Right-Sided Strokes: The Rotterdam Study. Stroke 46, 252–254. doi:10.1161/STROKEAHA.114.007385

Porter, F.D., Drago, J., Xu, Y., Cheema, S.S., Wassif, C., Huang, S.P., Lee, E., Grinberg, A., Massalas, J.S., Bodine, D., Alt, F., Westphal, H., 1997. Lhx2, a LIM homeobox gene, is required for eye, forebrain, and definitive erythrocyte development. Development 124, 2935–2944.

Portney, L., Watkins, M., 2007. Foundations of clinical research: applications to practice, 3rd ed. Prentice Hall.

Potter, G.M., Doubal, F.N., Jackson, C.A., Sudlow, C.L.M., Dennis, M.S., Wardlaw, J.M., 2012. Lack of association of white matter lesions with ipsilateral carotid artery stenosis. Cerebrovasc. Dis. 33, 378–384. doi:10.1159/000336762

Ragge, N.K., Brown, A.G., Poloschek, C.M., Lorenz, B., Henderson, R.A., Clarke, M.P., Russell-Eggitt, I., Fielder, A., Gerrelli, D., Martinez-Barbera, J.P., Ruddle, P., Hurst, J., Collin, J.R.O., Salt, A., Cooper, S.T., Thompson, P.J., Sisodiya, S.M., Williamson, K.A., Fitzpatrick, D.R., van Heyningen, V., Hanson, I.M., 2005. Heterozygous mutations of OTX2 cause severe ocular malformations. Am. J. Hum. Genet. 76, 1008–1022. doi:10.1086/430721

Randhawa, S., Shah, V.A., Kardon, R.H., 2007. Megalopapilla, not glaucoma. Arch. Ophthalmol. 125, 1134–1135. doi:10.1001/archopht.125.8.1134

Realini, T., Zangwill, L.M., Flanagan, J.G., Garway-Heath, D., Patella, V.M., Johnson, C.A., Artes, P.H., Gaddie, I.B., Fingeret, M., 2015. Normative Databases for Imaging Instrumentation. J. Glaucoma 24, 480–483. doi:10.1097/IJG.0000000000000152

Reis, L.M., Tyler, R.C., Schilter, K.F., Abdul-Rahman, O., Innis, J.W., Kozel, B.A., Schneider, A.S., Bardakjian, T.M., Lose, E.J., Martin, D.M., Broeckel, U., Semina, E. V, 2011. BMP4 loss-of-function mutations in developmental eye disorders including SHORT syndrome. Hum. Genet. 130, 495–504. doi:10.1007/s00439-011-0968-y

Relan, D., MacGillivray, T., Ballerini, L., Trucco, E., 2013. Retinal vessel classification: sorting

arteries and veins. Conf Proc IEEE Eng Med Biol Soc 2013, 7396–7399. doi:10.1109/embc.2013.6611267

Rizzoti, K., Lovell-Badge, R., 2007. SOX3 activity during pharyngeal segmentation is required for craniofacial morphogenesis. Development 134, 3437–3448. doi:10.1242/dev.007906

Saidha, S., Al-Louzi, O., Ratchford, J.N., Bhargava, P., Oh, J., Newsome, S.D., Prince, J.L., Pham, D., Roy, S., van Zijl, P., Balcer, L.J., Frohman, E.M., Reich, D.S., Crainiceanu, C., Calabresi, P.A., 2015. Optical coherence tomography reflects brain atrophy in multiple sclerosis: A four-year study. Ann Neurol 78, 801–813. doi:10.1002/ana.24487

Sampaolesi, R., Sampaolesi, J.R., 2001. Large optic nerve heads: megalopapilla or megalodiscs. Int. Ophthalmol. 23, 251–257.

Schneider, A., Bardakjian, T., Reis, L.M., Tyler, R.C., Semina, E. V, 2009. Novel SOX2 mutations and genotype-phenotype correlation in anophthalmia and microphthalmia. Am. J. Med. Genet. 149A, 2706–2715. doi:10.1002/ajmg.a.33098

Schwartz, R., Yatziv, Y., 2015. The effect of cataract surgery on ocular dominance. Clin. Ophthalmol. 9, 2329–2333. doi:10.2147/OPTH.S93142

Schwarz, M., Cecconi, F., Bernier, G., Andrejewski, N., Kammandel, B., Wagner, M., Gruss, P., 2000. Spatial specification of mammalian eye territories by reciprocal transcriptional repression of Pax2 and Pax6. Development 127, 4325–4334.

Shirodkar, C.G., Munta, K., Rao, S.M., Mahesh, M.U., 2015. Correlation of measurement of optic nerve sheath diameter using ultrasound with magnetic resonance imaging. Indian J. Crit. Care Med. 19, 466–470. doi:10.4103/0972-5229.162465

Spadea, L., Magni, R., Rinaldi, G., Dragani, T., Bianco, G., 1998. Unilateral retinitis pigmentosa: clinical and electrophysiological report of four cases. Ophthalmologica. 212, 350–354. doi:10.1159/000027324

Sposato, L., Cohen, G., Wardlaw, J., Sandercock, P., Lindley, R., Hachinski, V., 2016. Effect of Right Insular Involvement on Death and Functional Outcome after Acute Ischemic Stroke in the IST-3 Trial. Int. J. Stroke 47. doi:10.1161/STROKEAHA.116.014928

Staurenghi, G., Sadda, S., Chakravarthy, U., Spaide, R.F., for Optical Coherence Tomography Panel, I.N., 2014. Proposed lexicon for anatomic landmarks in normal posterior segment spectral-domain optical coherence tomography: the IN•OCT consensus. Ophthalmology

121, 1572–1578. doi:10.1016/j.ophtha.2014.02.023

Stroman, G.A., Stewart, W.C., Golnik, K.C., Curé, J.K., Olinger, R.E., 1995. Magnetic resonance imaging in patients with low-tension glaucoma. Arch. Ophthalmol. 113, 168–172. doi:10.1001/archopht.1995.01100020050027

Sugisaka, E., Ohde, H., Shinoda, K., Mashima, Y., 2007. Woman with atypical unilateral Leber's hereditary optic neuropathy with visual improvement. Clin. Experiment. Ophthalmol. 35, 868–870. doi:10.1111/j.1442-9071.2007.01628.x

Sullivan-Mee, M., Ruegg, C.C., Pensyl, D., Halverson, K., Qualls, C., 2013. Diagnostic precision of retinal nerve fiber layer and macular thickness asymmetry parameters for identifying early primary open-angle glaucoma. Am. J. Ophthalmol. 156, 567–577.e1. doi:10.1016/j.ajo.2013.04.037

Tatham, A.J., Medeiros, F.A., Zangwill, L.M., Weinreb, R.N., 2015. Strategies to improve early diagnosis in glaucoma. Prog. Brain Res. 221, 103–133. doi:10.1016/bs.pbr.2015.03.001

Tatham, A.J., Meira-Freitas, D., Weinreb, R.N., Marvasti, A.H., Zangwill, L.M., Medeiros, F.A., 2014. Estimation of retinal ganglion cell loss in glaucomatous eyes with a relative afferent pupillary defect. Invest. Ophthalmol. Vis. Sci. 55, 513–522. doi:10.1167/iovs.13-12921

Taylor, A.M., MacGillivray, T.J., Henderson, R.D., Ilzina, L., Dhillon, B., Starr, J.M., Deary, I.J., 2015. Retinal vascular fractal dimension, childhood IQ, and cognitive ability in old age: the Lothian Birth Cohort Study 1936. PLoS One 10, e0121119. doi:10.1371/journal.pone.0121119

Thakur, A., Puri, L., 2010. Unilateral retinitis pigmentosa. Clin. Exp. Optom. 93, 102–104. doi:10.1111/j.1444-0938.2009.00435.x

Thomson, K.L., Yeo, J.M., Waddell, B., Cameron, J.R., Pal, S., 2015. A systematic review and meta-analysis of retinal nerve fiber layer change in dementia, using optical coherence tomography. Alzheimer's Dement. Diagnosis, Assess. Dis. Monit. 1, 136–143. doi:10.1016/j.dadm.2015.03.001

Torgersen, J., 1950. Situs inversus, asymmetry, and twinning. Am. J. Hum. Genet. 2, 361–370.

Trucco, E., Ballerini, L., Relan, D., Giachetti, A., MacGillivray, T., Zutis, K., Lupascu, C., Tegolo, D., Pellegrini, E., Robertson, G., Wilson, P.J., Doney, A., Dhillon, B., 2013a. Novel VAMPIRE algorithms for quantitative analysis of the retinal vasculature, in: Biosignals and

Biorobotics Conference (BRC). pp. 1–4. doi:10.1109/BRC.2013.6487552

Trucco, E., Giachetti, A., Ballerini, L., Relan, D., Cavinato, A., MacGillivray, T., Joo-Hwee Lim, B., Ong, S.-H., Xiong, W., 2015. Morphometric measurements of the retinal vasculature in fundus images with Vampire, in: Lim, J.-H., Ong, S.-H., Xiong, W. (Eds.), Biomedical Image Understanding: Methods and Applications. John Wiley & Sons, Hoboken, pp. 91–111.

Trucco, E., Ruggeri, A., Karnowski, T., Giancardo, L., Chaum, E., Hubschman, J.P., Al-Diri, B., Cheung, C.Y., Wong, D., Abramoff, M., Lim, G., Kumar, D., Burlina, P., Bressler, N.M., Jelinek, H.F., Meriaudeau, F., Quellec, G., Macgillivray, T., Dhillon, B., 2013b. Validating retinal fundus image analysis algorithms: issues and a proposal. Invest Ophthalmol Vis Sci 54, 3546–3559. doi:10.1167/iovs.12-10347

Usrey, W.M., Alitto, H.J., 2015. Visual Functions of the Thalamus. Annu. Rev. Vis. Sci. 1, 351–371. doi:10.1146/annurev-vision-082114-035920

Valdés Hernández, M. del C., Maconick, L.C., Muñoz Maniega, S., Wang, X., Wiseman, S., Armitage, P.A., Doubal, F.N., Makin, S., Sudlow, C.L.M., Dennis, M.S., Deary, I.J., Bastin, M., Wardlaw, J.M., 2015. A comparison of location of acute symptomatic vs. “silent” small vessel lesions. Int. J. Stroke 10, 1044–1050. doi:10.1111/ijs.12558

Valdés Hernández, M. del C., Qiu, X., Wang, X., Wiseman, S., Sakka, E., Maconick, L.C., Doubal, F., Sudlow, C.L.M., Wardlaw, J.M., 2016. Interhemispheric characterization of small vessel disease imaging markers after subcortical infarct. Brain Behav. e00595. doi:10.1002/brb3.595

Verleger, R., Sprenger, A., Gebauer, S., Fritzmannova, M., Friedrich, M., Kraft, S., Jaśkowski, P., 2009. On Why Left Events are the Right Ones: Neural Mechanisms Underlying the Left-hemifield Advantage in Rapid Serial Visual Presentation. J. Cogn. Neurosci. 21, 474–488. doi:10.1162/jocn.2009.21038

Wallis, D.E., Roessler, E., Hehr, U., Nanni, L., Wiltshire, T., Richieri-Costa, A., Gillessen-Kaesbach, G., Zackai, E.H., Rommens, J., Muenke, M., 1999. Mutations in the homeodomain of the human SIX3 gene cause holoprosencephaly. Nat. Genet. 22, 196–198. doi:10.1038/9718

Wardlaw, J.M., Allerhand, M., Doubal, F.N., Hernandez, M.V., Morris, Z., Gow, A.J., Bastin, M., Starr, J.M., Dennis, M.S., Deary, I.J., 2014. Vascular risk factors, large-artery atheroma,

and brain white matter hyperintensities. Neurology 82, 1331–1338. doi:10.1212/WNL.0000000000000312

Wardlaw, J.M., Bastin, M.E., Valdés Hernández, M.C., Maniega, S.M., Royle, N.A., Morris, Z., Clayden, J.D., Sandeman, E.M., Eadie, E., Murray, C., Starr, J.M., Deary, I.J., 2011. Brain aging, cognition in youth and old age and vascular disease in the Lothian Birth Cohort 1936: rationale, design and methodology of the imaging protocol*. Int. J. Stroke 6, 547–559. doi:10.1111/j.1747-4949.2011.00683.x

Wardlaw, J.M., Smith, E.E., Biessels, G.J., Cordonnier, C., Fazekas, F., Frayne, R., Lindley, R.I., O'Brien, J.T., Barkhof, F., Benavente, O.R., Black, S.E., Brayne, C., Breteler, M., Chabriat, H., DeCarli, C., de Leeuw, F.E., Doubal, F., Duering, M., Fox, N.C., Greenberg, S., Hachinski, V., Kilimann, I., Mok, V., Oostenbrugge, R. van, Pantoni, L., Speck, O., Stephan, B.C.M., Teipel, S., Viswanathan, A., Werring, D., Chen, C., Smith, C., van Buchem, M., Norrving, B., Gorelick, P.B., Dichgans, M., 2013. Neuroimaging standards for research into small vessel disease and its contribution to ageing and neurodegeneration. Lancet Neurol. 12, 822–838. doi:10.1016/S1474-4422(13)70124-8

Watkins, K.E., Paus, T., Lerch, J.P., Zijdenbos, A., Collins, D.L., Neelin, P., Taylor, J., Worsley, K.J., Evans, A.C., 2001. Structural asymmetries in the human brain: a voxel-based statistical analysis of 142 MRI scans. Cereb. Cortex 11, 868–77. doi:10.1093/cercor/11.9.868

Watson, E.C., Koenig, M.N., Grant, Z.L., Whitehead, L., Trounson, E., Dewson, G., Coultas, L., 2016. Apoptosis regulates endothelial cell number and capillary vessel diameter but not vessel regression during retinal angiogenesis. Development 143, 2973–2982. doi:10.1242/dev.137513

Weller, J.M., Michelson, G., Juenemann, A.G., 2014. Unilateral retinitis pigmentosa: 30 years follow-up. BMJ Case Rep. 2014, 1–8. doi:10.1136/bcr-2013-202236

Wen, W., Pillai-Kastoori, L., Wilson, S.G., Morris, A.C., 2015. Sox4 regulates choroid fissure closure by limiting Hedgehog signaling during ocular morphogenesis. Dev. Biol. 399, 139–153. doi:10.1016/j.ydbio.2014.12.026

Werner, Y.L., Seifan, T., 2006. Eye size in geckos: Asymmetry, allometry, sexual dimorphism, and behavioral correlates. J. Morphol. 267, 1486–1500. doi:10.1002/jmor.10499

Wessel, J.M., Horn, F.K., Tornow, R.P., Schmid, M., Mardin, C.Y., Kruse, F.E., Juenemann, A.G., Laemmer, R., 2013. Longitudinal analysis of progression in glaucoma using spectral-

domain optical coherence tomography. Invest. Ophthalmol. Vis. Sci. 54, 3613–3620. doi:10.1167/iovs.12-9786

Wichmann, W., Müller-Forell, W., 2004. Anatomy of the visual system. Eur. J. Radiol. 49, 8–30. doi:10.1016/j.ejrad.2003.11.001

Williams, A.L., Gatla, S., Leiby, B.E., Fahmy, I., Biswas, A., de Barros, D.M., Ramakrishnan, R., Bhardwaj, S., Wright, C., Dubey, S., Lynch, J.F., Bayer, A., Khandelwal, R., Ichhpujani, P., Gheith, M., Siam, G., Feldman, R.M., Henderer, J.D., Spaeth, G.L., 2013. The value of intraocular pressure asymmetry in diagnosing glaucoma. J. Glaucoma 22, 215–218. doi:10.1097/IJG.0b013e318237bfb8

Wilson, S.I., Edlund, T., 2001. Neural induction: toward a unifying mechanism. Nat. Neurosci. 4 Suppl, 1161–1168. doi:10.1038/nn747

Wiltschko, W., Traudt, J., Güntürkün, O., Prior, H., Wiltschko, R., 2002. Lateralization of magnetic compass orientation in a migratory bird. Nature 419, 467–470. doi:10.1038/nature00958

Wiltschko, W., Wiltschko, R., 1988. Magnetic orientation in birds. Curr. Ornithol. 5, 67–121. doi:10.1007/978-1-4615-6787-5_2

Wong, A.C.M., Chan, C.W.N., Hui, S.P., 2005. Relationship of Gender, Body Mass Index, and Axial Length with Central Retinal Thickness Using Optical Coherence Tomography. Eye 19, 292–297. doi:10.1038/sj.eye.6701466

Wong, T.Y., Klein, R., Klein, B.E.K., Meuer, S.M., Hubbard, L.D., 2003. Retinal vessel diameters and their associations with age and blood pressure. Invest. Ophthalmol. Vis. Sci. 44, 4644–4650. doi:10.1167/iovs.03-0079

Wong, T.Y., Knudtson, M.D., Klein, R., Klein, B.E.K., Meuer, S.M., Hubbard, L.D., 2004. Computer-assisted measurement of retinal vessel diameters in the Beaver Dam Eye Study: methodology, correlation between eyes, and effect of refractive errors. Ophthalmology 111, 1183–1190. doi:10.1016/j.ophtha.2003.09.039

Wong, T.Y., Wong, T., Mitchell, P., 2007. The eye in hypertension. Lancet 369, 425–435. doi:10.1016/S0140-6736(07)60198-6

Worrall, D., Wilson, C., Brostow, G., 2016. Automated Retinopathy of Prematurity Case Detection with Convolutional Neural Networks, in: Carneiro, G. (Ed.), International

Workshop on Large-Scale Annotation of Biomedical Data and Expert Label Synthesis. Springer International, Athens, pp. 68–76.

Yang, M., Wang, W., Xu, Q., Tan, S., Wei, S., 2016. Interocular symmetry of the peripapillary choroidal thickness and retinal nerve fibre layer thickness in healthy adults with isometropia. BMC Ophthalmol. 16, 182. doi:10.1186/s12886-016-0361-7

Yantis, S., Schwarzbach, J., Serences, J.T., Carlson, R.L., Steinmetz, M.A., Pekar, J.J., Courtney, S.M., 2002. Transient neural activity in human parietal cortex during spatial attention shifts. Nat. Neurosci. 5, 995–1002. doi:10.1038/nn921

Yu-Wai-Man, P., Griffiths, P.G., Burke, A., Sellar, P.W., Clarke, M.P., Gnanaraj, L., Ah-Kine, D., Hudson, G., Czermin, B., Taylor, R.W., Horvath, R., Chinnery, P.F., 2010. The prevalence and natural history of dominant optic atrophy due to OPA1 mutations. Ophthalmology 117, 1538–1546. doi:10.1016/j.ophtha.2009.12.038

Yu-Wai-Man, P., Griffiths, P.G., Chinnery, P.F., 2011. Mitochondrial optic neuropathies – Disease mechanisms and therapeutic strategies. Prog. Retin. Eye Res. 30, 81–114. doi:10.1016/j.preteyeres.2010.11.002

Zayed, H., Chao, R., Moshrefi, A., Lopezjimenez, N., Delaney, A., Chen, J., Shaw, G.M., Slavotinek, A.M., 2010. A maternally inherited chromosome 18q22.1 deletion in a male with late-presenting diaphragmatic hernia and microphthalmia-evaluation of DSEL as a candidate gene for the diaphragmatic defect. Am. J. Med. Genet. 152A, 916–923. doi:10.1002/ajmg.a.33341

Zhou, M., Lu, B., Zhao, J., Wang, Q., Zhang, P., Sun, X., 2016. Interocular symmetry of macular ganglion cell complex thickness in young Chinese subjects. PLoS One 11, e0159583. doi:10.1371/journal.pone.0159583

Zuber, M.E., Perron, M., Philpott, A., Bang, A., Harris, W.A., 1999. Giant eyes in Xenopus laevis by overexpression of XOptx2. Cell 98, 341–352. doi:10.1016/S0092-8674(00)81963-7